

Hiroshima University Doctoral Thesis

**Neutrinos and lepton number
oscillations in quantum field
theory**

(場の量子論に基づく
ニュートリノとレプトン数振動)

2022

Department of Physics,
Graduate School of Science,
Hiroshima University

Benoit, Nicholas James

Table of Contents

1. Main Thesis

Neutrinos and lepton number oscillations in quantum field theory

(場の量子論に基づくニュートリノとレプトン数振動)

Benoit, Nicholas James

2. Articles

(1) Time Evolution of Lepton Number Carried by Majorana Neutrinos

A. S. Adam, **N. J. Benoit**, Y. Kawamura, Y. Matsuo, T. Morozumi,

Y. Shimizu, Y. Tokunaga and N. Toyota

..... Prog. Theor. Exp. Phys. **2021**, 053B01.

Part I
Main Thesis

Abstract

Neutrino physics has changed significantly since the discovery of flavor oscillations by Super Kamiokande and the Sudbury Neutrino Observatory. Starting with the work of Pontecovo, the theory of neutrino flavor oscillations in quantum mechanics has been established for some time. However, a consensus for the theory of neutrino flavor oscillations in quantum field theory has not been reached and is an active area of research.

We developed a formulation of neutrino flavor oscillations based on lepton family numbers in quantum field theory. We will start with a derivation of lepton family number for neutrinos with Majorana masses. Then, we will derive the lepton family number for neutrinos with Dirac masses. The main result of those derivations are a Majorana expectation value from our original work and a Dirac expectation value that is new for this thesis.

Some important results from of the expectation values are time dependent oscillations, total lepton number violation or conservation, and the recovery of the quantum mechanics formulation in the ultra-relativistic limit. We also compare the Majorana expectation value and the Dirac expectation value, which is a new comparison for this thesis. We compare them in two ways, first by studying the total lepton number and second by comparing the low momentum phenomenology. For total lepton number, we find the Dirac expectation value to conserve total lepton number, whereas the Majorana expectation value violates total lepton number. In the low momentum phenomenology our formulation has three interesting properties, we can distinguish the neutrino mass type, differences from the neutrino mass hierarchy are enhanced, and the Majorana phases can play an important role to the Majorana Expectation value.

Lastly, we prove our formulation is the same in the Schrödinger and Heisenberg pictures. We study a non-trivial relationship between the Fock spaces of the operators, which is not usually considered in high energy physics. That non-trivial relationship leads to a Bogolyubov transformation that connects the operators of the Fock spaces. This is sometimes considered in Thermal field theory and gives an interesting theoretical background to our model.

Contents

I	Main Thesis	3
1	Introduction to neutrino physics	3
1.1	Brief history of neutrinos	3
1.1.1	Fermi Theory and Parity	4
1.1.2	Lepton families and number	5
1.2	Neutrinos in the Standard Model	6
1.3	Neutrino flavor oscillations	8
1.3.1	Super-Kamiokande and the Sudbury Neutrino Observatory	9
1.3.2	Neutrino flavor oscillations in quantum mechanics	10
1.3.3	Breakdown of the ultrarelativistic approximation	12
1.3.4	Neutrino flavor oscillations in Quantum Field Theory	14
1.4	Open questions and prospects	17
2	Framework for the lepton number carried by neutrinos	18
2.1	Single flavor Majorana neutrinos	19
2.2	Lepton number for Majorana neutrinos	21
2.2.1	Time evolution of the lepton family numbers . . .	26
2.2.2	Comparison to the quantum mechanic formulation	28
2.3	Lepton number for Dirac neutrinos	34
2.3.1	Time evolution of Dirac family numbers	39
3	Comparison of Majorana and Dirac Expectation Values	43
3.1	Total Lepton Number	44
3.2	Phenomenology of the lepton family numbers	47
3.3	Summary	52
4	Lepton number in the Schrödinger picture	53
4.1	Unitarily inequivalent representations	54
4.2	The Bogolyubov transformation	55

4.3	Expectation value in the Schrödinger picture	58
5	Conclusions	61
A	Parameterization of the unitary mixing matrix	65
B	Regions of the momentum	68
B.1	The continuity condition	68
B.2	The momentum regions	69

Chapter 1

Introduction to neutrino physics

Neutrinos are one of the most interesting particles in our universe. They are the only known particle to break from the Standard Model. This comes from the results of neutrino oscillations experiments, for example Super Kamiokande [1, 2, 3] and NOvA [4, 5, 6], requiring massive neutrinos. Neutrino oscillation phenomenon has grown into a vast field, originating with the work of Pontecovo and quantum mechanics [47]. Nowadays, there are numerous experiments that aim to take precision measurements within the next ten years. Some of these measurements include:

- Neutrino mass hierarchy,
- Neutrino mass type,
- CP violation in the leptonic sector,
- Absolute mass scale of the neutrinos.

In spite of the numerous precision experiments, the theory of neutrino oscillations is not fully established.

1.1 Brief history of neutrinos

This is not an exhaustive review, for more details on the history of neutrinos please see the database at neutrino-history.in2p3.fr and the references [7, 9, 8].

In the late 19th century a kind of radioactive decay called β -decay was discovered. Today, we know β -decay is the release of an electron e^- from the atomic nucleus; at that time it was understood as $A \rightarrow B + \beta^-$, where A is the parent and B is the daughter nuclei. The electron and atomic nucleus are known to have a fixed mass, so studies of β -decay expected the released electron to be monoenergetic. However, multiple experiments found the electron energy to be smoothly distributed [10, 11] that lead to two possible explanations.

1. Energy was only conserved in a statistical sense for atomic processes,
2. Or some other, unmeasurable, particle was involved in β -decay [12].

For the second explanation, an unmeasurable particle would have to be electrically neutral otherwise it could be measured with the same techniques as the electron. At that time no electrically neutral particles were known. In addition, to reproduce the smooth distribution of β -decay energies it would have to be effectively massless. These concepts lead Fermi to the name neutrino, which is derived from Italian for little (effectively massless), neutral one (electrically neutral) [13].

Around the 1930s it was discussed whether neutrinos were undetectable [14]. Nevertheless, in 1946 Pontecorvo proposed a method to detect neutrinos that is called Inverse β -decay [15]. Inverse β -decay is the interaction between an electron antineutrino and the proton that produces a neutron and positron, $\bar{\nu}_e + p \rightarrow n + e^+$. Such an experiment would have to detect the neutron and the positron. Ten years after the proposal by Pontecorvo, the neutrino was experimentally discovered by Reines and Cowan using inverse β -decay [16]. The discovery of the neutrino removed the idea that energy is not exactly conserved for atomic processes.

1.1.1 Fermi Theory and Parity

The first quantum theory of nuclear β -decays was formulated by Fermi starting in the year 1934 [17]. He described β -decays as a four fermion interaction with the rate being suppressed by an overall constant term G_f . At the time, Fermi theory was analogous with the new theory of quantum electrodynamics (QED) and Fermi theory formed the beginning of neutrino physics.

Gamow and Teller extended Fermi theory with a parity conserving axial-vector interaction [18]. Furthermore, Pontecorvo suggested Fermi theory should also apply to the newly discovered muons [19] and about this time β -decays started to be generalized into the Weak Interaction. Perhaps famously, Fermi theory is nonrenormalizable and is only accurate for energies near the nuclear mass range.

After the experimental discovery of parity violation in the Weak Interaction [20, 21], the theory for Weak Interactions became more complicated. The complications arose as the Gamow and Teller model had to be extended with parity violating interactions that greatly increased the allowed interaction structures. Many people worked to remedy those complications, coalescing in the formulation of $V - A$ theory [22, 23, 24, 25, 26, 27]. To achieve the $V - A$ interaction, the neutrinos are massless left-handed fermions and antineutrinos are massless right-handed fermions.

1.1.2 Lepton families and number

After Pontecorvo suggested Fermi theory should be applied to both electrons and muons, the concept of Lepton families started to appear [28, 29, 30, 31]. It was until 1953 that Konopinski and Mahmoud introduced the more modern notation of lepton number L [32], and today we use their notation to write the following assignments,

$$\begin{array}{cccccc|l} e^- & \nu_e & \mu^- & \nu_\mu & \tau^- & \nu_\tau & L = +1 \\ e^+ & \bar{\nu}_e & \mu^+ & \bar{\nu}_\mu & \tau^+ & \bar{\nu}_\tau & L = -1 \end{array}$$

The lepton numbers are then broken down into families denoted by the charged leptons,

$$\begin{array}{cc|l} e^- & \nu_e & L_e = +1 \\ \mu^- & \nu_\mu & L_\mu = +1 \\ \tau^- & \nu_\tau & L_\tau = +1. \end{array}$$

These assignments for lepton number and lepton family number mean that L is a conserved value in $V - A$ theory, and forbids the processes $\mu \rightarrow e + \gamma$ and $\bar{\nu}_e + {}^{37}\text{Cl} \rightarrow {}^{37}\text{Ar} + e^-$. The first process of $\mu \rightarrow e + \gamma$ breaks lepton family number conservation as the muon is assigned $L_\mu = +1$ and electron is assigned $L_e = +1$. So the muon family in that process is nonzero, implying family violation, similarly for the electron family. The second process of $\bar{\nu}_e + {}^{37}\text{Cl} \rightarrow {}^{37}\text{Ar} + e^-$ breaks lepton number conservation for the anti-electron neutrino minus the

electron is nonzero $(+1) - (-1) = 2$. Schwartz used lepton family number conservation to prove the existence of the muon neutrino in 1962, in an experiment suggested by Pontecorvo [33, 34].

1.2 Neutrinos in the Standard Model

The next big step for neutrino physics occurred in 1961, when Glashow incorporated the $V - A$ theory with quantum electrodynamics in an $SU(2) \times U(1)$ gauge model [35]. Then Weinberg and Salam included the Higgs mechanism in the Glashow model to produce the Glashow-Weinberg-Salam Standard Model (SM) [36, 37]. In the Standard Model, neutrinos are only involved with the electroweak interactions. They are left-handed massless fermions described as Weyl fields often denoted ν_α taken from $V - A$ theory, where $\alpha = e, \mu, \tau$ marks the lepton family or flavor.

The electroweak Lagrangian in the Standard Model is summarized as,

$$\mathcal{L}_\nu = -i \sum_\alpha \bar{l}_{\alpha L} \not{D} l_{\alpha L} + \text{h.c.}, \quad (1.1)$$

which involves left-handed neutrinos in the lepton $SU(2)$ doublet,

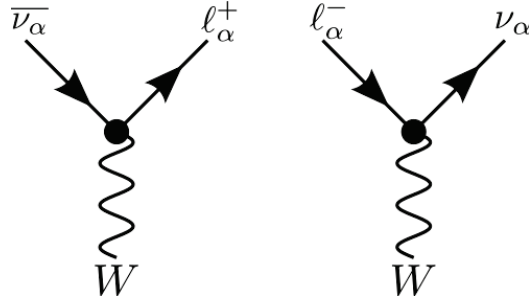
$$l_{\alpha L} = \begin{pmatrix} \nu_{\alpha L} \\ \alpha_L \end{pmatrix}. \quad (1.2)$$

Right-handed neutrinos are not included, the same as $V - A$ theory. We can expand the covariant derivative of Eq.(1.1) $D = \partial_\mu + igA_\mu \cdot I + ig' B_\mu \frac{Y}{2}$ into kinetic and interaction sections. The interaction section describes how neutrinos couple with the weak interaction gauge bosons W and Z,

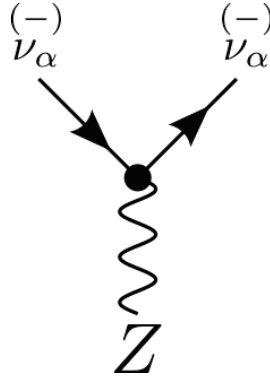
$$\mathcal{L}_{\nu,I}^{CC} = - \sum_\alpha \frac{g}{\sqrt{2}} (\bar{\nu}_{\alpha L} \gamma^\rho l_{\alpha L} W_\rho + \text{h.c.}), \quad (1.3)$$

$$\mathcal{L}_{\nu,I}^{NC} = - \sum_\alpha \frac{g}{2 \cos \vartheta_W} \bar{\nu}_{\alpha L} \gamma^\rho \nu_{\alpha L} Z_\rho. \quad (1.4)$$

The charged current (CC) interaction of Eq.(1.3) with the W-Boson are direct replacements of Fermi theory and $V - A$ theory. The original Fermi constant, G_f , is replaced by the interaction coupling g divided by the mass of the W-Boson m_W resulting in the relation $G_f = (g^2 \sqrt{2}) / (8m_W^2)$. The Feynman diagrams for the charged current interactions are,



The neutral current (NC) interaction of Eq.(1.4) with the Z-Boson are new in the Standard Model. For neutrinos, the Feynman diagram for the neutral current interaction is,



Similar to the charged current interactions, the Fermi constant can be derived from a four fermion interaction that exchanges a Z-Boson. The result is the relation $G_f = (g^2\sqrt{2})/(8\cos^2\vartheta_W m_Z^2)$. Practically, the Standard Model inherits the electrically neutral and massless neutrinos from the $V - A$ and Fermi theories.

In 1973, muon neutrinos were measured to have been scattered off electrons and nucleons by the neutral current interaction at the Gargamelle experiment [38, 39, 40]. The Gargamelle results helped to validate the neutral current and Standard Model, cementing the importance of the neutrino. Another important experiment for neutrinos in the Standard Model is a measurement of the effective number of neutrino flavors via the decay width of the Z-boson. The effective number of flavors is measured from the invisible decay of the Z-boson,

$$\Gamma_{\text{inv}} = \Gamma_Z - (\Gamma_{\text{hadron}} + \Gamma_{\tau\tau} + \Gamma_{\mu\mu} + \Gamma_{ee}). \quad (1.5)$$

If we assume only Standard Model particles, then the invisible decay is written $\Gamma_{\text{inv}} = N_\nu \Gamma_{\nu\bar{\nu}}$ where N_ν is the effective number of flavors.

The most precise measurement was done by the LEP experiment and concluded only three flavors of neutrinos exist, section 7.2.2 of [41].

Electric neutrality often poses a problem for experiments, because the only probe available for neutrinos are the weak interactions, which have very small cross-sections. For that reason neutrinos are not experimentally measured unless it is done by a dedicated experiment. Instead, experiments treat neutrinos as missing energy whose degrees-of-freedom (DOF) are integrated over, as was the case for the LEP experiment. This has led neutrinos to be the least experimentally understood fermions in the Standard Model.

1.3 Neutrino flavor oscillations

Even though neutrinos are the least understood fermions, they are also the only experimentally confirmed particles to be beyond the Standard Model. This fact came to light starting in the late 1960s with the Homestake experiment, which was designed to measure electron neutrinos from nuclear fusion in the sun [42]. The experiment was designed to capture the neutrinos with chlorine ^{37}Cl and transform into an isotope of argon ^{37}Ar ,



Then, after some weeks the argon could be extracted and measured, which would be directly correlated to the number of neutrino events. Rather famously, only about a third of the expected argon was measured [43]. This led to years of research into solar modeling and repeated experiments at Homestake.

Simultaneously in the 1980s, the Kamiokande experiment was searching for proton decays predicted by numerous Grand Unified Theories (GUTs). Proton decay is a signature of GUTs and is physics beyond the Standard Model following the general form,



where the neutral pion decays into two photons $\pi^0 \rightarrow 2\gamma$. How the positron and pion is produced depend on the details of the exact GUT model.

To perform a proton decay search, the Kamiokande experiment had to develop software that could distinguish proton decay from atmospheric neutrino interactions of ν_μ and ν_e . Their software was able

to distinguish simple atmospheric neutrino interactions easily and predictions for the number of events was created; however, when the software was applied to experimental data the number of ν_μ events was fewer than predictions [44]. Investigations of the software found no issues and the neutrino deficit was suggested to be real measurement.

Before the Homestake experiment, in 1958, Pontecorvo suggested electron neutrinos could oscillate to electron antineutrinos $\nu_e \rightleftharpoons \bar{\nu}_e$ [45, 46]. Primarily, he based his work on neutral Kaon oscillations $K^0 \rightleftharpoons \bar{K}^0$ that had been experimentally discovered. After the Homestake experiment results were released, he offered a solution to the ν_e deficit based on his particle-antiparticle oscillation work. His solution assumed neutrinos were massive particles that oscillated between flavors $\nu_e \rightleftharpoons \nu_\mu$ not particle-antiparticles [47, 48]. Unknown to him, neutrino flavor oscillations had been separately discussed by Maki, Nakagawa and Sakata a few years before [49].

Neutrino flavor oscillations were also taken up by the Kamiokande experiment as a possible solution to their measured ν_μ deficit. However, neither the Homestake nor the Kamiokande experiment was statistically significant enough to warrant any conclusions. In addition, the flavor oscillations proposed by Pontecorvo could not explain the all the Homestake experiment ν_e deficit.

1.3.1 Super-Kamiokande and the Sudbury Neutrino Observatory

The next generation of experiments were built with the intention of measuring the same neutrinos as Kamiokande and Homestake. There were two main experiments focused on those neutrinos,

- Super-Kamiokande,
- Sudbury Neutrino Observatory (SNO).

Super-Kamiokande is a larger version of the Kamiokande experiment and used the larger volume to increase the number of measured ν_μ events. More measured events meant a smaller statistical uncertainty. The Sudbury Neutrino Observatory was a superseding version of the Homestake experiment and was able to measure all neutrino flavors ν_e , ν_μ , and ν_τ . Importantly, Super-Kamiokande reported above 5-sigma deficits in ν_μ compared to the Standard Model expected value

and the Sudbury Neutrino Observatory reported no deficits when all the neutrino flavors were summed. But, the Sudbury Neutrino Observatory reported the same deficit as the Homestake experiment in ν_e and enhancements in ν_μ and ν_τ . Both results strongly favored a neutrino flavor oscillation solution [50, 51].

As a note, for both experiments to realize their results the flavor oscillations proposed by Pontecorvo, Maki, Nakagawa, and Sakata (PMNS) had to be extended. Mikheev, Smirnov, and Wolfenstein (MSW) accomplished the extension by modifying the oscillation phases with potential effects from propagation through matter [52, 53, 54]. Super-Kamiokande used the MSW effect, or matter effect, to measure differences in neutrino fluxes coming from above vs below the detector. The fluxes of neutrinos observed by the Sudbury Neutrino Observatory were modified by matter in the sun.

1.3.2 Neutrino flavor oscillations in quantum mechanics

This will be a brief review of how neutrino flavor oscillations are formulated in quantum mechanics. For a detailed discussion see the works of [8, 9, 55, 56]. We assume the neutrinos are already produced in a charged current weak interaction similar to Eq.(1.3). The flavor of the neutrino is defined by the $SU(2)$ lepton pair. These flavors are denoted with Greek symbols $\alpha = e, \mu, \tau$;

$$|\nu_\alpha\rangle = \sum_i U_{\alpha i}^* |\nu_i\rangle, \quad (1.8)$$

where from the weak interaction the PMNS matrix $U_{\alpha i}$ is unitary and the massive neutrino states are orthonormal $\langle \nu_j | \nu_i \rangle = \delta_{ji}$ ¹. A brief overview of the PMNS matrix is in appendix A. We do not completely constrain the number of massive neutrino states $i \geq 3$. In the flavor basis, states above three are called sterile neutrinos, because any states above three would not participate in the weak interaction. In this way, since sterile neutrinos do not participate in the weak interaction they avoid the effective number measured by the LEP experiment [41].

Next, we treat the massive neutrino states as eigenstates of the Hamiltonian,

$$\mathcal{H}|\nu_i\rangle = E_i(\vec{p})|\nu_i\rangle. \quad (1.9)$$

¹Throughout our work the Greek indices will represent flavor and the Latin indices will represent massive states.

That Hamiltonian evolves according to the Schrödinger equation and leads to a time evolution solution for the massive neutrino states,

$$|\nu_i(t)\rangle = e^{-iE_i(\vec{p})t} |\nu_i\rangle \quad (1.10)$$

We desire the time evolution in the flavor basis, so we use Eq.(1.8) and the unitary property of the PMNS matrix to write,

$$\begin{aligned} |\nu_\alpha(t)\rangle &= \sum_i U_{\alpha i}^* e^{-iE_i(\vec{p})t} |\nu_i\rangle \\ &= \sum_\beta \left(\sum_i U_{\alpha i}^* e^{-iE_i(\vec{p})t} U_{\beta i} \right) |\nu_i\rangle. \end{aligned} \quad (1.11)$$

We highlight that at $t = 0$ the flavor neutrino state of Eq.(1.11) is a pure flavor i.e., $\alpha = e, \mu, \tau$ due to the unitary properties of the PMNS matrix. Then for $t > 0$ the pure state becomes a superposition of flavor states. The transition probability of an initial flavor state α to be changed into a new state β is calculated as,

$$\begin{aligned} P_{\alpha \rightarrow \beta}(t) &= |\langle \nu_\beta | \nu_\alpha(t) \rangle|^2 \\ &= \sum_{i,j} U_{\alpha i}^* U_{\beta i} U_{\alpha j} U_{\beta j}^* e^{-i(E_i(\vec{p}) - E_j(\vec{p}))t}, \end{aligned} \quad (1.12)$$

where the phase of the oscillations are the energy differences $\phi_{i,j} = -(E_i(\vec{p}) - E_j(\vec{p}))t$. Typically, experiments are run for neutrinos that satisfy $|\vec{p}| \gg m_{i,j}$, which leads to the three ultrarelativistic approximations:

1. The dispersion relation of the massive neutrino eigenstates becomes $E_i(\vec{p}) \simeq |\vec{p}| + m_i^2/|\vec{p}|$.
2. The average energy is defined as $E = |\vec{p}|$.
3. The time evolution is rewritten as the distance from the neutrino source to the detector $t = L$.

The ultrarelativistic approximation transforms Eq.(1.12) the transition probability to be,

$$P_{\alpha \rightarrow \beta}(t) \simeq \sum_{i,j} U_{\alpha i}^* U_{\beta i} U_{\alpha j} U_{\beta j}^* \exp \left[-i \frac{\Delta m_{i,j}^2 L}{2E} \right], \quad (1.13)$$

where $\Delta m_{i,j}^2 \equiv (m_i^2 - m_j^2)$ is the squared mass differences. Some important facts about Eq.(1.13), the elements of the PMNS matrix and the

squared mass differences are measured by experiments as described at the end of appendix A. In contrast, the macroscopic distance L and the energy E of the experiments are known. When we sum over α or β the probability is conserved, equal to unity, because of the unitary property of the PMNS matrix. Lastly, Eq.(1.12) and Eq.(1.13) tell us neutrino flavor oscillations are periodic changes in flavor described by mass dependent phases and amplitudes. This is interesting, because no external influence is required to have a flavor transition.

1.3.3 Breakdown of the ultrarelativistic approximation

From the beginning the ultrarelativistic approximation was scrutinized and questioned [56, 60, 61, 62, 63, 64]. To list a few of the questions:

- When is the approximation applicable?
- Is energy-momentum conservation broken by oscillations?
- When are oscillations expected to be observed?

Let us briefly explore why these questions appear following the argument of Giunti and Kim [56]. When we consider a pion decay at rest following $\pi \rightarrow \mu + \nu$ the four momentum conservation leads to,

$$E_k^2 = \frac{m_\pi^2}{4} \left(1 - \frac{m_\mu^2}{m_\pi^2}\right)^2 + \frac{m_k^2}{2} \left(1 - \frac{m_\mu^2}{m_\pi^2}\right) + \frac{m_k^4}{4m_\pi^2}, \quad (1.14)$$

$$p_k^2 = \frac{m_\pi^2}{4} \left(1 - \frac{m_\mu^2}{m_\pi^2}\right)^2 - \frac{m_k^2}{2} \left(1 + \frac{m_\mu^2}{m_\pi^2}\right) + \frac{m_k^4}{4m_\pi^2}, \quad (1.15)$$

where m_k is the mass of the neutrino mass eigenstates. If we neglect the m_k^4 terms, because the neutrino masses are tiny compared to the pion and muon, the conservation equations are rewritten as,

$$E_k \simeq A + \eta \frac{m_k^2}{2A}, \quad (1.16)$$

$$p_k \simeq A - (1 - \eta) \frac{m_k^2}{2A}. \quad (1.17)$$

For the pion decay to a muon and neutrino, A and η take on the values of,

$$A = \frac{m_\pi}{2} \left(1 - \frac{m_\mu^2}{m_\pi^2} \right) \simeq 30 \text{ MeV}, \quad (1.18)$$

$$\eta = \frac{1}{2} \left(1 - \frac{m_\mu^2}{m_\pi^2} \right) \simeq 0.2. \quad (1.19)$$

When deriving the transition probability of Eq.(1.13) we assumed the neutrino mass eigenstates have the same momentum \vec{p} and defined the average energy to be $E = |\vec{p}|$. For the mass eigenstates to have the same momentum, the four component conservation equation of Eq.(1.17) tells us $\eta = 1$. Clearly, this is contradictory to the value of $\eta \simeq 0.2$ for conservation in the pion decay at rest. Even if we change the decay channel to be $\pi \rightarrow e + \nu$ for a pion at rest, the four component conservation gives $\eta \simeq 0.5$, which is not the same as our assumptions for Eq.(1.13) tell us. We conclude that the assumptions leading to Eq.(1.13) break energy-momentum conservation, and we should consider when Eq.(1.13) is applicable.

The resolution to these questions is found by considering wave packet for the neutrinos, as opposed to plane waves. Details on wave packets in quantum mechanics can be found in the beginning of older textbooks [65, 66].

In the most general sense, wave packets are localized expressions built with interfering plain waves that can be expressed,

$$\psi(\vec{x}, t) = \int d\vec{k} f(\vec{k} - \vec{k}_0) e^{i\vec{k} \cdot \vec{x} - iE(\vec{k})t}, \quad (1.20)$$

where $f(k - k_0)$ is called the damping function, or weighting function. See figure 1.1 for an example, the plain waves have constructive and destructive interference. This leads to a localized wave function. For neutrino flavor oscillations, wave packets modify the oscillation formula of Eq.(1.13) with additional terms related to energy-momentum conservation and damping from decoherence. We rewrite Eq.(1.11) in terms of a wave packet,

$$|\nu_\alpha(t)\rangle = \sum_i U_{\alpha i}^* \psi_i(\vec{x}, t) |\nu_i\rangle. \quad (1.21)$$

The wave function $\psi_i(\vec{x}, t)$ is different for each mass eigenstate. The damping factor $f_i(\vec{k} - \vec{k}_0)$ inside the wave function, acts to introduce

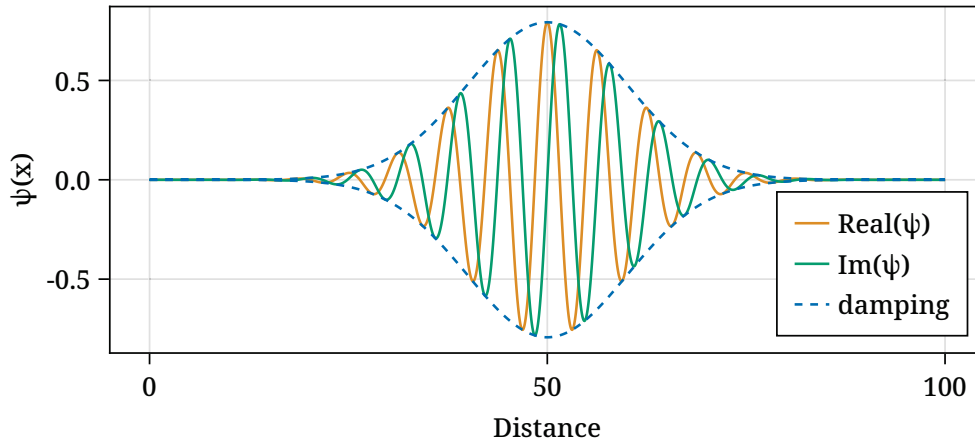


Figure 1.1: Example of wave packet where the damping function is Gaussian. The plane wave parts are enveloped by the damping function.

quantum uncertainties into the energy-momentum of the mass eigenstates. This modifies Eq.(1.12) and Eq.(1.13) to account for $\eta \neq 1$ from Eq.(1.16) and Eq.(1.17). Details of the resulting transition probability can be found in the work of Giunti and Kim [56].

Presently experiments have not observed effects due to wave packets, and the ultrarelativistic approximation is enough to explain their data.

1.3.4 Neutrino flavor oscillations in Quantum Field Theory

The use of Quantum Field Theory to describe neutrino flavor oscillations is more diverse than Quantum Mechanics [67, 68]. To list a few there are external wave packet models (virtual propagator models [69, 70, 71, 72] and real propagator models [74, 73]), source-propagator models [75, 76, 77], and the weak Fock space model (Blasone-Vitiello model) [78, 79, 80, 81, 82, 83]. All of those models reproduce the Quantum Mechanics derived oscillation formula Eq.(1.12) in some limit, but are in general different from each other.

The original motivation to use Quantum Field Theory was to resolve the issues of energy-momentum conservation and investigate if the assumptions of the Quantum Mechanics derivation are reasonable.

We will not give a full proof in the Quantum Field Theory formulation, but instead we will summarize the results of an external wave packet model. Please refer to the review by Beuthe [68] or the textbook by Giunti and Kim [8] for a complete proof.

External wave packet models are formulated with the neutrino detection and production processes. All the detection and production particles are treated as wave packets, often Gaussian, with asymptotic initial and final states;

$$|f_P\rangle = \mathcal{S}|P_I\rangle \quad \text{production,} \quad (1.22)$$

$$|f_D\rangle = \mathcal{S}|\nu, D_I\rangle \quad \text{detection,} \quad (1.23)$$

where \mathcal{S} is the process S-matrix. At this point, we must consider the details of the production and detection processes to define $|f_P\rangle$ and $|f_D\rangle$. If, for example, we consider the production of a neutrino and then detection of a neutrino following lepton number conservation;

$$P_I \rightarrow P_F + l_\alpha^+ + \nu_\alpha^P \quad \text{production,} \quad (1.24)$$

$$\nu_\alpha^D + D_I \rightarrow D_F + l_\alpha^- \quad \text{detection,} \quad (1.25)$$

are general processes that could occur. Then we can identify the state $|f_P\rangle = \sum_j \mathcal{A}_{\alpha j}^P |\nu_j, l_\alpha^+, P_F\rangle$, where the coefficient $\mathcal{A}_{\alpha j}^P$ is the amplitude of production for this process. To solve for the neutrino flavor state we take the projection,

$$|\nu_\alpha^P\rangle = \langle P_F, l_\alpha^+ | f_P \rangle = \sum_j \langle P_F, l_\alpha^+ | \mathcal{A}_{\alpha j}^P | \nu_j, l_\alpha^+, P_F \rangle, \quad (1.26)$$

which becomes the equation,

$$|\nu_\alpha^P\rangle = \frac{1}{N^P} \sum_j \mathcal{A}_{\alpha j}^P |\nu_j\rangle \quad (1.27)$$

with the normalization $N^P = \sqrt{\sum_k |\mathcal{A}_{\alpha k}^P|^2}$. A similar kind of formula can be found for the detection process,

$$|\nu_\alpha^D\rangle = \frac{1}{N^D} \sum_j \mathcal{A}_{\alpha j}^D |\nu_j\rangle. \quad (1.28)$$

Neutrino flavor oscillations occur over a spacetime interval from the production location to the detection location. To represent that we evolve the production state Eq.(1.27) in spacetime,

$$|\nu_\alpha(\mathbf{L}, t)\rangle = e^{-i(q^0 t - \mathbf{q} \cdot \mathbf{L})} |\nu_\alpha^P\rangle, \quad (1.29)$$

where we have assumed the neutrinos to have a definite energy and momentum². The transition amplitude for the measured process $\nu_\alpha \rightarrow \nu_\beta$ is found by bringing Eq.(1.28) in from the left,

$$\begin{aligned} A_{\alpha \rightarrow \beta}(\mathbf{L}, t) &= \langle \nu_\beta^D | \nu_\alpha(\mathbf{L}, t) \rangle \\ &= \langle \nu_\beta^D | e^{-i(q^0 t - \mathbf{q} \cdot \mathbf{L})} | \nu_\alpha^P \rangle \\ &= \frac{1}{\mathbf{N}^P \mathbf{N}^D} \sum_j \mathcal{A}_{\alpha j}^P \mathcal{A}_{\beta j}^{D*} e^{-i(E_j t - \mathbf{q}_j \cdot \mathbf{L})}. \end{aligned} \quad (1.30)$$

For simplicity, we now consider the evolution to only occur in one spatial dimension writing $\mathbf{q}_j \cdot \mathbf{L} \approx q_j L$. Then the probability for the transition $\nu_\alpha \rightarrow \nu_\beta$ to occur is,

$$\begin{aligned} P_{\alpha \rightarrow \beta}(L, t) &= |A_{\alpha \rightarrow \beta}(L, t)|^2 \\ &= \frac{1}{(\mathbf{N}^P \mathbf{N}^D)^2} \sum_{j,k} \mathcal{A}_{\alpha j}^P \mathcal{A}_{\beta j}^{D*} \mathcal{A}_{\alpha k}^{P*} \mathcal{A}_{\beta k}^D e^{i\Phi_{jk}}, \end{aligned} \quad (1.31)$$

where the oscillation phase $\Phi_{jk} = -((E_j - E_k)t - (q_j - q_k)L)$ is the same as the Quantum Mechanical version of Eq.(1.12). In fact, if we take the ultrarelativistic approximation of $t = L$ then $-E_j t + q_j L = -(m_j^2 L)/(E_j + q_j) \simeq -(m_j^2 L)/(2E)$, and the oscillation phase becomes;

$$\Phi_{jk} \simeq -\frac{\Delta m_{j,k}^2 L}{2E}. \quad (1.32)$$

The approximated phase is exactly the same as the Quantum Mechanical approximation Eq.(1.13).

Differences between the Quantum Mechanical and the external wave packet results are two modifications to the oscillation amplitudes.

1. The external wave packet amplitude is suppressed by normalization factors \mathbf{N}^P and \mathbf{N}^D .
2. The amplitude is modified by the production $\mathcal{A}_{\alpha j}^P$ and detection $\mathcal{A}_{\beta k}^D$ amplitudes.

To understand those two modification we must consider the charged current interaction of Eq.(1.3). We do not go into details here, but after

²Proper treatment of the evolution should be done for energy momentum distributions of the production and detection particles described with wave packets.

considering the charged current interaction Eq.(1.27) and Eq.(1.28) are rewritten as;

$$|\nu_\alpha^P\rangle = \sum_j \frac{\mathcal{M}_{\alpha j}^P}{\sqrt{\sum_k |U_{\alpha k}|^2 |\mathcal{M}_{\alpha k}^P|^2}} U_{\alpha j}^* |\nu_j\rangle, \quad (1.33)$$

$$|\nu_\alpha^D\rangle = \sum_j \frac{\mathcal{M}_{\alpha j}^D}{\sqrt{\sum_k |U_{\alpha k}|^2 |\mathcal{M}_{\alpha k}^D|^2}} U_{\alpha j}^* |\nu_j\rangle. \quad (1.34)$$

The symbols $\mathcal{M}_{\alpha j}^{(P,D)}$ are the matrix elements of the production and detection charged current processes. Ultimately, this means the probability of Eq.(1.31) is written as,

$$P_{\alpha \rightarrow \beta}(L, t) = \sum_{j,k} \frac{\mathcal{M}_{\alpha j}^P \mathcal{M}_{\alpha k}^{P*}}{\sum_i |U_{\alpha i}|^2 |\mathcal{M}_{\alpha i}^P|^2} \frac{\mathcal{M}_{\beta j}^D \mathcal{M}_{\beta k}^{D*}}{\sum_i |U_{\beta i}|^2 |\mathcal{M}_{\beta i}^D|^2} \times U_{\alpha j}^* U_{\beta j} U_{\alpha k} U_{\beta k}^* e^{-i[(E_j - E_k)t - (q_j - q_k)L]}. \quad (1.35)$$

In summary, the external wave packet model modifies the quantum mechanic probability with corrections from the production and detection processes.

1.4 Open questions and prospects

Neutrino physics has evolved significantly since the discovery of flavor oscillations by Super Kamiokande [50] and the Sudbury Neutrino Observatory [51]. Nowadays, there are numerous experiments that aim to take precision measurements within the next ten years. Some measurements include:

- Neutrino mass hierarchy,
- Neutrino mass type,
- CP violation in the leptonic sector,
- Absolute mass scale of the neutrinos.

Furthermore, the originating work of Pontecovo with neutrino oscillations in quantum mechanics [47] has been established to not be a theoretically complete model for neutrino oscillations. And, a consensus for the theory of neutrino oscillations in quantum field theory has not been reached. In the next chapter, chapt. 2, we will discuss in detail how we have contributed to the discussion of neutrino oscillations in quantum field theory.

Chapter 2

Framework for the lepton number carried by neutrinos

We consider a formulation of neutrino flavor oscillations based on lepton family numbers in quantum field theory. As we introduced in section 1.1.2, lepton family numbers are conserved values in $V - A$ theory and are a $U(1)$ global symmetry in the Standard Model. However, an implication of neutrino flavor oscillations is lepton family number violation [8]. That implication is an important connection, for neutrino flavor oscillations, between the quantum mechanics of section 1.3.2 and quantum field theory of section 1.3.4.

Equally important is what occurs for total lepton number after the neutrino mass type is considered, as a reminder total lepton number is the sum over all the lepton family numbers. For example, if we assign neutrinos to have a Majorana mass type then the total lepton number would be violated. However, if we assign a Dirac mass type, the total lepton number is conserved. The reason for a difference in total lepton number can be seen from inspecting the mass construction,

$$m_D \underbrace{\overline{\psi_R} \psi_L}_{-1+1=0} \quad \text{Dirac mass,} \quad (2.1)$$

$$\frac{1}{2} m_M \underbrace{\overline{\psi_L^C} \psi_L}_{1+1=2} \quad \text{Majorana mass,} \quad (2.2)$$

where the subscripts are counting the lepton numbers for a single flavor and $\psi_L^C = (\psi_L)^C$. If a particle is described with a Majorana field $\psi_M = \psi_L + \psi_L^C$ the electromagnetic current $j^\mu = q \overline{\psi_M} \gamma^\mu \psi_M$ vanishes. This means only an electrically neutral particle can be a Majorana field and in the Standard Model, only the neutrino is electrically neutral.

We are interested in how the different mass types effect neutrino oscillations, as the current quantum mechanics and quantum field theory models provide no incite. Furthermore, we think the effect of the different mass types on total lepton number will be reflected in the flavor oscillations. To illustrate our ideas in a simple way, first we will consider a model with only one flavor.

2.1 Single flavor Majorana neutrinos

We write the single flavor Majorana Lagrangian as,

$$\mathcal{L}^S = \bar{\nu}_L i \gamma^\mu \partial_\mu \nu_L - \theta(t) \left(\frac{m_M}{2} \bar{\nu}_L^C \nu_L + \text{h.c.} \right), \quad (2.3)$$

where we have used the notation $\nu_L^C = (\nu_L)^C$ for charge conjugation and the subscript L denotes the left-handed projection operator $P_L = (1 - \gamma^5)/2$. The Lagrangian of Eq.(2.3) has the structure where the first term is the kinetic part and the second term is the Majorana mass part. A step-function $\theta(t)$ controls the second term and separates the Lagrangian into two regions. In the first region, we approach the zero time from below until we are infinitesimally away,

$$\lim_{t \rightarrow 0^-} t = -\epsilon. \quad (2.4)$$

For that region, the fields of Eq.(2.3) are Fourier expanded as Weyl spinors,

$$\nu_L(-\epsilon, \mathbf{x}) = \int' \frac{d^3 \mathbf{p}}{(2\pi)^3 2|\mathbf{p}|} (a(\mathbf{p}) u_L(\mathbf{p}) e^{i\mathbf{p}\cdot\mathbf{x}} + b^\dagger(\mathbf{p}) v_L(\mathbf{p}) e^{-i\mathbf{p}\cdot\mathbf{x}}). \quad (2.5)$$

The creation and annihilation operators obey the usual anti-commutation relations,

$$\{a(\mathbf{p}), a^\dagger(\mathbf{q})\} = \{b(\mathbf{p}), b^\dagger(\mathbf{q})\} = 2|\mathbf{p}| (2\pi)^3 \delta^{(3)}(\mathbf{p} - \mathbf{q}), \quad (2.6)$$

with all others being zero. We constrain the left-handed spinors $u_L(\mathbf{p})$ and $v_L(\mathbf{p})$ to be normalized as,

$$u_L(\mathbf{p}) = -v_L(\mathbf{p}) = \sqrt{|2\mathbf{p}|} \begin{pmatrix} 0 \\ \phi_-(\mathbf{n}) \end{pmatrix}, \quad (2.7)$$

$$\mathbf{n} \cdot \boldsymbol{\sigma} \phi_\pm(\mathbf{n}) = \pm \phi_\pm(\mathbf{n}), \quad (2.8)$$

$$\mathbf{n} = \frac{\mathbf{p}}{|\mathbf{p}|}. \quad (2.9)$$

The symbol σ denotes a vector of the Pauli matrices. We use the integral notation of \int' to denote the regions of $\{\mathbf{p} \neq 0, \mathbf{p} \in A, -\mathbf{p} \in \bar{A}\}$ with details in appendix B.

We approach the zero time from above in the second region delimited by the step-function,

$$\lim_{t \rightarrow 0^+} t = +\epsilon. \quad (2.10)$$

In this region, the neutrinos are Majorana fermions that are Fourier expanded to be,

$$P_L \nu(+\epsilon, \mathbf{x}) = P_L \int' \frac{d^3 \mathbf{p}}{(2\pi)^3 2E(\mathbf{p})} \sum_{\lambda=\pm} (a_M(\mathbf{p}, \lambda) u(\mathbf{p}, \lambda) e^{i\mathbf{p}\cdot\mathbf{x}} + a_M^\dagger(\mathbf{p}, \lambda) v(\mathbf{p}, \lambda) e^{-i\mathbf{p}\cdot\mathbf{x}}), \quad (2.11)$$

where $E(\mathbf{p}) = \sqrt{\mathbf{p}^2 + m^2}$, λ is the spinor helicity, and $P_L = (1 - \gamma^5)/2$ is the left-handed projection operator. Again the creation and annihilation operators obey the relation,

$$\{a_M(\mathbf{p}, \lambda), a_M^\dagger(\mathbf{q}, \lambda')\} = 2E(\mathbf{p})(2\pi)^3 \delta^{(3)}(\mathbf{p} - \mathbf{q}) \delta_{\lambda\lambda'}, \quad (2.12)$$

and all others are zero. Next, we use the continuity condition described in appendix B to relate the two regions of the step-function,

$$\nu_L(-\epsilon, \mathbf{x}) = P_L \nu(+\epsilon, \mathbf{x}). \quad (2.13)$$

This results in relations for the operators of Eq.(2.5) and Eq.(2.11),

$$\begin{pmatrix} a(\mathbf{p}) \\ a^\dagger(-\mathbf{p}) \end{pmatrix} = \frac{\sqrt{2|\mathbf{p}|N(\mathbf{p})}}{2E(\mathbf{p})} \begin{pmatrix} 1 & i\frac{m}{N(\mathbf{p})} \\ i\frac{m}{N(\mathbf{p})} & 1 \end{pmatrix} \begin{pmatrix} a_M(\mathbf{p}, -) \\ a_M^\dagger(-\mathbf{p}, -) \end{pmatrix}, \quad (2.14)$$

$$\begin{pmatrix} b(\mathbf{p}) \\ b^\dagger(-\mathbf{p}) \end{pmatrix} = \frac{\sqrt{2|\mathbf{p}|N(\mathbf{p})}}{2E(\mathbf{p})} \begin{pmatrix} 1 & i\frac{m}{N(\mathbf{p})} \\ i\frac{m}{N(\mathbf{p})} & 1 \end{pmatrix} \begin{pmatrix} a_M(\mathbf{p}, +) \\ a_M^\dagger(-\mathbf{p}, +) \end{pmatrix}. \quad (2.15)$$

We have used the notation of $N(\mathbf{p}) = E(\mathbf{p}) + |\mathbf{p}|$. We find the time evolution form of the operators by writing $a_M(\mathbf{p}, \lambda)$ as $a_M(\mathbf{p}, \lambda) e^{-iE(\mathbf{p})t}$ and using the operator relations of Eq.(2.14) and Eq.(2.15) to write

$a_M(\mathbf{p}, \lambda)$ in terms of $a(\mathbf{p})$:

$$\begin{pmatrix} a(\mathbf{p}, t) \\ a^\dagger(-\mathbf{p}, t) \end{pmatrix} = \begin{bmatrix} \cos E(\mathbf{p})t & \begin{pmatrix} 1 & 0 \\ 0 & 1 \end{pmatrix} \\ -i \sin E(\mathbf{p})t & \begin{pmatrix} v & -i\sqrt{1-v^2} \\ i\sqrt{1-v^2} & -v \end{pmatrix} \end{bmatrix} \begin{pmatrix} a(\mathbf{p}) \\ a^\dagger(-\mathbf{p}) \end{pmatrix}, \quad (2.16)$$

$$\begin{pmatrix} b(\mathbf{p}, t) \\ b^\dagger(-\mathbf{p}, t) \end{pmatrix} = \begin{bmatrix} \cos E(\mathbf{p})t & \begin{pmatrix} 1 & 0 \\ 0 & 1 \end{pmatrix} \\ -i \sin E(\mathbf{p})t & \begin{pmatrix} v & -i\sqrt{1-v^2} \\ i\sqrt{1-v^2} & -v \end{pmatrix} \end{bmatrix} \begin{pmatrix} a(\mathbf{p}) \\ a^\dagger(-\mathbf{p}) \end{pmatrix}. \quad (2.17)$$

For the single flavor case we define the lepton number to be a Heisenberg operator of the form,

$$L^S(t) = \int_{\mathbf{p} \in A} (a^\dagger(\mathbf{p}, t)a(\mathbf{p}, t) - b^\dagger(\mathbf{p}, t)b(\mathbf{p}, t) + a^\dagger(-\mathbf{p}, t)a(-\mathbf{p}, t) - b^\dagger(-\mathbf{p}, t)b(-\mathbf{p}, t)). \quad (2.18)$$

Then we prepare a normalized state such that,

$$|\nu_L(\mathbf{q})\rangle = \frac{a^\dagger(\mathbf{q})|0\rangle}{\sqrt{\langle 0|a(\mathbf{q})a^\dagger(\mathbf{q})|0\rangle}}, \quad (2.19)$$

which we sandwich around Eq.(2.18) the single flavor operator. After substituting Eq.(2.16) and Eq.(2.17) we have a single flavor expectation value that oscillates in time,

$$\langle \nu_L(\mathbf{q})|L^S|\nu_L(\mathbf{q})\rangle = v^2 + (1 - v^2) \cos 2E(\mathbf{q})t. \quad (2.20)$$

As a final note, this oscillation is directly proportional to the mass of the neutrino though the term $(1 - v^2) = m_M^2/(E(\mathbf{q}))$. When we consider the momenta to be greater than the neutrino mass, the amplitude of the oscillations decreases, until we reach the ultra-relativistic limit and all oscillations become negligible.

2.2 Lepton number for Majorana neutrinos

Next, we consider the following multi-flavor Lagrangian for Majorana neutrinos,

$$\mathcal{L}^M = i\overline{\psi_{L\alpha}}\gamma^\mu\partial_\mu\psi_{L\alpha} - \theta(t) \left(\frac{m_{\alpha\beta}}{2}\overline{\psi_{L\alpha}^C}\psi_{L\beta} + \text{h.c.} \right). \quad (2.21)$$

This Lagrangian has the same structure and notation as Eq.(2.3) the single flavor case. The first term is the usual kinetic term and the second term is the multi-flavor Majorana mass. We have included a time-dependent step-function, $\theta(t)$, in the second term to guarantee an initial pure flavor state i.e., $\alpha = e, \mu, \tau$.

A difference between the single and multi-flavor is the diagonalization process. The multi-flavor, Majorana mass matrix is complex and symmetric, so we can use the Takagi factorization for the diagonalization [85],

$$m_k \delta_{kj} = (U^T)_{k\alpha} m_{\alpha\beta} U_{\beta j}, \quad (2.22)$$

$$\psi_{L\alpha} = U_{\alpha k} \psi_{Lk}. \quad (2.23)$$

Which uses a unitary matrix U for the diagonalization. Then, using the Majorana field $\psi_k = \psi_{Lk} + \psi_{Lk}^C$ we rewrite the Lagrangian of Eq.(2.21) when the mass matrix is diagonal,

$$\mathcal{L}^M = i \frac{1}{2} \overline{\psi_k} \gamma^\mu \partial_\mu \psi_k - \theta(t) \frac{m_k}{2} \overline{\psi_k} \psi_k. \quad (2.24)$$

Notice, the mass term is still separated by the step-function $\theta(t)$.

We use the step-function to separate two regions in our formulation. Then, we relate those two regions by continuity of the fields. In the first region, we approach the zero time from below until reaching an infinitesimal distance away,

$$\lim_{t \rightarrow 0^-} t = -\epsilon. \quad (2.25)$$

There we Fourier expand the neutrino fields of Eq.(2.21) as Weyl fermions,

$$\psi_{L\alpha}(-\epsilon, \mathbf{x}) = \int' \frac{d^3 \mathbf{p}}{(2\pi)^3 2|\mathbf{p}|} (a_\alpha(\mathbf{p}) u_L(\mathbf{p}) e^{i\mathbf{p}\cdot\mathbf{x}} + b_\alpha^\dagger(\mathbf{p}) v_L(\mathbf{p}) e^{-i\mathbf{p}\cdot\mathbf{x}}). \quad (2.26)$$

We constrain the left-handed spinors $u_L(\mathbf{p})$ and $v_L(\mathbf{p})$ such that they obey the conditions,

$$u_L(\mathbf{p}) = -v_L(\mathbf{p}) = \sqrt{2|\mathbf{p}|} \begin{pmatrix} 0 \\ \phi_-(\mathbf{n}) \end{pmatrix}, \quad (2.27)$$

$$\mathbf{n} \cdot \boldsymbol{\sigma} \phi_\pm(\mathbf{n}) = \pm \phi_\pm(\mathbf{n}), \quad (2.28)$$

$$\mathbf{n} = \frac{\mathbf{p}}{|\mathbf{p}|}. \quad (2.29)$$

The symbol σ denotes a vector of the Pauli matrices. In addition, the integral notation of \int' denotes regions allowed for the momentum $\{\mathbf{p} \neq 0, \mathbf{p} \in A, -\mathbf{p} \in \bar{A}\}$ with details in appendix B. The momentum regions appear in the spinors as the following,

$$\phi_+(\mathbf{n}) = \begin{pmatrix} e^{i\frac{\phi}{2}} \cos \frac{\theta}{2} \\ e^{-i\frac{\phi}{2}} \sin \frac{\theta}{2} \end{pmatrix}, \quad (2.30)$$

$$\phi_-(\mathbf{n}) = \begin{pmatrix} -e^{i\frac{\phi}{2}} \sin \frac{\theta}{2} \\ e^{-i\frac{\phi}{2}} \cos \frac{\theta}{2} \end{pmatrix}, \quad (2.31)$$

$$\phi_+(-\mathbf{n}) = \begin{pmatrix} -ie^{i\frac{\phi}{2}} \sin \frac{\theta}{2} \\ ie^{-i\frac{\phi}{2}} \cos \frac{\theta}{2} \end{pmatrix}, \quad (2.32)$$

$$\phi_-(-\mathbf{n}) = \begin{pmatrix} ie^{i\frac{\phi}{2}} \cos \frac{\theta}{2} \\ ie^{-i\frac{\phi}{2}} \sin \frac{\theta}{2} \end{pmatrix}. \quad (2.33)$$

The phases of the spinors are adjusted such that $\phi_{\pm}(\mathbf{n}) = \pm i\sigma^2 \phi_{\mp}^*(\mathbf{n})$. Lastly, the operators of Eq.(2.26) from the Fourier expansion obey the usual anti-commutation relations,

$$\left. \begin{array}{l} \{a_{\alpha}(\mathbf{p}), a_{\beta}^{\dagger}(\mathbf{q})\} \\ \{b_{\alpha}(\mathbf{p}), b_{\alpha}^{\dagger}(\mathbf{q})\} \end{array} \right\} = 2|\mathbf{p}|(2\pi)^3 \delta^{(3)}(\mathbf{p} - \mathbf{q}) \delta_{\alpha\beta}, \quad (2.34)$$

with all other relations being zero.

For the second region delimited by the step-function, we approach the zero time from above,

$$\lim_{t \rightarrow 0^+} t = +\epsilon. \quad (2.35)$$

For this region, the neutrinos are Majorana fermions that are Fourier expanded to be,

$$U_{\alpha k} \psi_{Lk}(+\epsilon, \mathbf{x}) = U_{\alpha k} P_L \int' \frac{d^3 \mathbf{p}}{(2\pi)^3 2E_k(\mathbf{p})} \sum_{\lambda=\pm} \left(a_{Mk}(\mathbf{p}, \lambda) u_k(\mathbf{p}, \lambda) e^{i\mathbf{p}\cdot\mathbf{x}} + a_{Mk}^{\dagger}(\mathbf{p}, \lambda) v_k(\mathbf{p}, \lambda) e^{-i\mathbf{p}\cdot\mathbf{x}} \right), \quad (2.36)$$

where $E_k(\mathbf{p}) = \sqrt{\mathbf{p}^2 + m_k^2}$ is the energy of each mass state, λ is the spinor helicity, and $P_L = (1 - \gamma^5)/2$ is the left-handed projection opera-

tor. We normalize the spinors so that they have definite helicities,

$$u_k(\mathbf{p}, +) = \sqrt{E_k(\mathbf{p}) + |\mathbf{p}|} \begin{pmatrix} \phi_+(\mathbf{n}) \\ \frac{m_k}{E_k(\mathbf{p}) + |\mathbf{p}|} \phi_+(\mathbf{n}) \end{pmatrix}, \quad (2.37)$$

$$u_k(\mathbf{p}, -) = \sqrt{E_k(\mathbf{p}) + |\mathbf{p}|} \begin{pmatrix} \frac{m_k}{E_k(\mathbf{p}) + |\mathbf{p}|} \phi_-(\mathbf{n}) \\ \phi_-(\mathbf{n}) \end{pmatrix}, \quad (2.38)$$

$$v_k(\mathbf{p}, +) = \sqrt{E_k(\mathbf{p}) + |\mathbf{p}|} \begin{pmatrix} \frac{m_k}{E_k(\mathbf{p}) + |\mathbf{p}|} \phi_-(\mathbf{n}) \\ -\phi_-(\mathbf{n}) \end{pmatrix}, \quad (2.39)$$

$$v_k(\mathbf{p}, -) = \sqrt{E_k(\mathbf{p}) + |\mathbf{p}|} \begin{pmatrix} -\phi_+(\mathbf{n}) \\ \frac{m_k}{E_k(\mathbf{p}) + |\mathbf{p}|} \phi_+(\mathbf{n}) \end{pmatrix}. \quad (2.40)$$

Again, the integral notation of \int' denotes regions allowed for the momentum with details in appendix B. The momentum regions are the same for the spinors as Eq.(2.30) to Eq.(2.33). In addition, they obey the usual orthogonality and completeness relations,

$$u_k^\dagger(\mathbf{p}, \lambda) u_k(\mathbf{p}, \lambda') = v_k^\dagger(-\mathbf{p}, \lambda) v_k(-\mathbf{p}, \lambda') = \delta_{\lambda\lambda'}, \quad (2.41)$$

$$\sum_{\lambda} \left(u_k^\dagger(\mathbf{p}, \lambda) u_k(\mathbf{p}, \lambda') + v_k^\dagger(-\mathbf{p}, \lambda) v_k(-\mathbf{p}, \lambda') \right) = 1. \quad (2.42)$$

Lastly, the operator $a_{Mk}(\mathbf{p}, \lambda)$ of Eq.(2.36) is distinct from the operators of Eq.(2.26). Sometimes we will call $a_{Mk}(\mathbf{p}, \lambda)$ the Majorana operators, and they obey the anti-commutation relation,

$$\{a_{Mk}(\mathbf{p}, \lambda), a_{Mj}^\dagger(\mathbf{q}, \lambda')\} = 2E(\mathbf{p})(2\pi)^3 \delta^{(3)}(\mathbf{p} - \mathbf{q}) \delta_{kj} \delta_{\lambda\lambda'}, \quad (2.43)$$

with all others being zero.

The two regions separated by the step-function of Eq.(2.21) are connected by continuity of the equation of motion. This can be seen after integrating the equation of motion derived from Eq.(2.21) over an infinitesimal time interval,

$$\int_{-\epsilon}^{+\epsilon} dt \frac{\partial \psi_{L\alpha}}{\partial t} = - \int_{-\epsilon}^{+\epsilon} dt \gamma^0 \gamma^i \frac{\partial \psi_{L\alpha}}{\partial x^i} \psi_{L\alpha} - i \int_0^{+\epsilon} dt \gamma^0 m_{\alpha\beta}^* \gamma^0 \psi_{L\beta}^C. \quad (2.44)$$

We reexpress the continuity in terms of the fields Eq.(2.26) and Eq.(2.36),

$$\lim_{\epsilon \rightarrow 0^+} \psi_{L\alpha}(-\epsilon, \mathbf{x}) = \lim_{\epsilon \rightarrow 0^+} U_{\alpha i} L \psi_i(+\epsilon, \mathbf{x}). \quad (2.45)$$

The details of the calculation are in appendix B. The continuity condition allows us to write relations between the operators $a_{L\alpha}(\mathbf{p})$ and

$b_{L\alpha}^\dagger(\mathbf{p})$ of Eq.(2.26) with the Majorana operators $a_{Mi}(\mathbf{p}, \lambda)$ and $a_{Mi}^\dagger(\mathbf{p}, \lambda)$ of Eq.(2.36).

$$a_\alpha(\mathbf{p}) = U_{\alpha k} \frac{\sqrt{2|\mathbf{p}|N_k(\mathbf{p})}}{2E_k(\mathbf{p})} \left(a_{Mk}(\mathbf{p}, -) + \frac{im_k}{N_k(\mathbf{p})} a_{Mk}^\dagger(-\mathbf{p}, -) \right), \quad (2.46)$$

$$b_\alpha(\mathbf{p}) = U_{\alpha k} \frac{\sqrt{2|\mathbf{p}|N_k(\mathbf{p})}}{2E_k(\mathbf{p})} \left(a_{Mk}(\mathbf{p}, +) + \frac{im_k}{N_k(\mathbf{p})} a_{Mk}^\dagger(-\mathbf{p}, +) \right), \quad (2.47)$$

where $N_k(\mathbf{p}) = E_k(\mathbf{p}) + |\mathbf{p}|$. Notice, the relations are a non-trivial mixing of the Majorana annihilation and creation operators forming $a_\alpha(\mathbf{p})$ and $b_\alpha(\mathbf{p})$. Naively, we may have expected the relations to only depend on the Majorana annihilation operators. In addition, compared to the single flavor case of Eq.(2.14) and Eq.(2.15), the multi-flavored relations depend on the PMNS matrix $U_{\alpha k}$ because of the Takagi factorization Eq.(2.22). We will use Eq.(2.46) and Eq.(2.47) to assist with solving for the time evolution of $a_\alpha(\mathbf{p})$ and $b_\alpha(\mathbf{p})$.

For the time evolution, we are interested in region two where the neutrinos are massive Majorana fields. So, we write Eq.(2.26) as $U_{\alpha k} \psi_{Lk}(t, \mathbf{x})$, which indicates the operator is multiplied by the time evolution to become,

$$a_{Mk}(\mathbf{p}, \lambda) \rightarrow a_{Mk}(\mathbf{p}, \lambda) e^{-iE_k(\mathbf{p})t}, \quad (2.48)$$

$$a_{Mk}^\dagger(\mathbf{p}, \lambda) \rightarrow a_{Mk}^\dagger(\mathbf{p}, \lambda) e^{iE_k(\mathbf{p})t}. \quad (2.49)$$

Then Eq.(2.46) and Eq.(2.47) become time dependent,

$$a_\alpha(t, \mathbf{p}) = U_{\alpha k} \frac{\sqrt{2|\mathbf{p}|N_k(\mathbf{p})}}{2E_k(\mathbf{p})} \left(a_{Mk}(\mathbf{p}, -) e^{-iE_k(\mathbf{p})t} + \frac{im_k}{N_k(\mathbf{p})} a_{Mk}^\dagger(-\mathbf{p}, -) e^{iE_k(\mathbf{p})t} \right), \quad (2.50)$$

$$b_\alpha(t, \mathbf{p}) = U_{\alpha k} \frac{\sqrt{2|\mathbf{p}|N_k(\mathbf{p})}}{2E_k(\mathbf{p})} \left(a_{Mk}(\mathbf{p}, +) e^{-iE_k(\mathbf{p})t} + \frac{im_k}{N_k(\mathbf{p})} a_{Mk}^\dagger(-\mathbf{p}, +) e^{iE_k(\mathbf{p})t} \right). \quad (2.51)$$

Our goal is to write the time evolution solely in terms of the operators $a_\alpha(\mathbf{p})$ and $b_\alpha(\mathbf{p})$. So we use the operator relations of Eq.(2.46) and Eq.(2.47), derived from the continuity condition, as substitutions for the operators $a_{Mk}(\mathbf{p}, \lambda)$ and $a_{Mk}^\dagger(\mathbf{p}, \lambda)$ of Eq.(2.50) and Eq.(2.51). Then,

we expand the time dependent exponential into sine and cosine components, and identify that $|\mathbf{p}|/E_k(\mathbf{p}) = v_k$ and $m_k/E_k(\mathbf{p}) = \sqrt{1 - v_k^2}$,

$$a_\alpha(t, \mathbf{p}) = \sum_{\beta=e}^{\tau} \sum_k \left(U_{\alpha k} U_{\beta k}^* [\cos E_k(\mathbf{p})t - i v_k \sin E_k(\mathbf{p})t] a_\beta(\mathbf{p}) - i U_{\alpha k} U_{\beta k} \sqrt{1 - v_k^2} \sin[E_k(\mathbf{p})t] a_\beta^\dagger(-\mathbf{p}) \right), \quad (2.52)$$

$$b_\alpha(t, \mathbf{p}) = \sum_{\gamma=e}^{\tau} \sum_j \left(U_{\alpha j}^* U_{\gamma j} [\cos E_j(\mathbf{p})t - i v_j \sin E_j(\mathbf{p})t] b_\gamma(\mathbf{p}) - i U_{\alpha j}^* U_{\gamma j} \sqrt{1 - v_j^2} \sin[E_j(\mathbf{p})t] b_\gamma^\dagger(-\mathbf{p}) \right), \quad (2.53)$$

These relations are a cornerstone of our work, and again we would like to highlight the non-trivial mixing of the operators. The non-trivial mixing will lead to phenomena similar to neutrino flavor oscillations. We will derive how that phenomena occurs in section 2.2.1, and then we will discuss how it compares to the quantum mechanic and quantum field theory models from chapter 1 in section 2.2.2.

2.2.1 Time evolution of the lepton family numbers

We assign lepton family numbers based on the charged lepton in the $SU(2)_L$ doublet from the weak interaction L_e, L_μ, L_τ . The lepton family numbers are Heisenberg operators treated as,

$$L_\alpha^M(t) = \int d^3x : \overline{\psi}_{L\alpha}(t, \mathbf{x}) \gamma^0 \psi_{L\alpha}(t, \mathbf{x}) :, \quad (2.54)$$

where $\alpha = e, \mu$, and τ and $::$ denotes normal ordering with respect to the $a_\alpha(\mathbf{p})$ and $b_\alpha(\mathbf{p})$ vacuum. We substitute in the time dependent form of Eq.(2.26), then take the integral over space. The lepton family numbers are then written in terms of time dependent operators,

$$L_\alpha^M(t) = \int' \frac{d^3p}{(2\pi)^3 |2\mathbf{p}|} (a_\alpha^\dagger(t, \mathbf{p}) a_\alpha(t, \mathbf{p}) - b_\alpha^\dagger(t, \mathbf{p}) b_\alpha(t, \mathbf{p})). \quad (2.55)$$

As a reminder, the integral notation of \int' denotes regions allowed for the momentum $\{\mathbf{p} \neq 0, \mathbf{p} \in A, -\mathbf{p} \in \overline{A}\}$ with details in appendix B. To relocate the time dependency outside the operators, we use Eq.(2.52) and Eq.(2.53) that we found using the continuity condition. The result

is the lepton family numbers written in terms of the time independent operators,

$$\begin{aligned}
L_\alpha^M(t) = & \int' \frac{d\mathbf{p}}{(2\pi)^3 |2\mathbf{p}|} \sum_{\beta\gamma} \sum_{kj} \\
& \times \left[(A_{\beta\gamma}(+, \mathbf{p}) U_{\alpha k}^* U_{\beta k} U_{\alpha j} U_{\gamma j}^* - B_{\beta\gamma}(+, \mathbf{p}) U_{\alpha k} U_{\beta k}^* U_{\alpha j}^* U_{\gamma j}) \right. \\
& \times (\cos E_k(\mathbf{p})t \cos E_j(\mathbf{p})t + v_k v_j \sin E_k(\mathbf{p})t \sin E_j(\mathbf{p})t \\
& \quad + i v_k \sin E_k(\mathbf{p})t \cos E_j(\mathbf{p})t - i v_j \cos E_k(\mathbf{p})t \sin E_j(\mathbf{p})t) \\
& - (A_{\beta\gamma}(-, \mathbf{p}) U_{\alpha k}^* U_{\beta k} U_{\alpha j} U_{\gamma j} - B_{\beta\gamma}(-, \mathbf{p}) U_{\alpha k} U_{\beta k}^* U_{\alpha j}^* U_{\gamma j}^*) \\
& \times \left(\sqrt{1 - v_j^2} \cos E_k(\mathbf{p})t \sin E_j(\mathbf{p})t + i v_k \sqrt{1 - v_j^2} \sin E_k(\mathbf{p})t \sin E_j(\mathbf{p})t \right) \\
& + (A_{\beta\gamma}(-, \mathbf{p}) U_{\alpha k}^* U_{\beta k}^* U_{\alpha j} U_{\gamma j} - B_{\beta\gamma}(-, \mathbf{p}) U_{\alpha k} U_{\beta k} U_{\alpha j}^* U_{\gamma j}^*) \\
& \times \left(\sqrt{1 - v_k^2} \cos E_j(\mathbf{p})t \sin E_k(\mathbf{p})t + i v_j \sqrt{1 - v_k^2} \sin E_j(\mathbf{p})t \sin E_k(\mathbf{p})t \right) \\
& - (A_{\gamma\beta}(+, \mathbf{p}) U_{\alpha k}^* U_{\beta k}^* U_{\alpha j} U_{\gamma j} - B_{\gamma\beta}(+, \mathbf{p}) U_{\alpha k} U_{\beta k} U_{\alpha j}^* U_{\gamma j}^*) \\
& \left. \times \sqrt{1 - v_k^2} \sqrt{1 - v_j^2} \sin E_k(\mathbf{p})t \sin E_j(\mathbf{p})t \right]
\end{aligned} \tag{2.56}$$

where we have used the notation $A_{\gamma\beta}(\pm, \mathbf{p}) = a_\gamma^\dagger(\mathbf{p})a_\beta(\mathbf{p}) \pm a_\gamma^\dagger(-\mathbf{p})a_\beta(-\mathbf{p})$ and $B_{\gamma\beta}(\pm, \mathbf{p}) = b_\gamma^\dagger(\mathbf{p})b_\beta(\mathbf{p}) \pm b_\gamma^\dagger(-\mathbf{p})b_\beta(-\mathbf{p})$.

To further study the time evolution, we take the expectation value of Eq.(2.56) the operator for the lepton family numbers. We prepare a normalized single flavor state, $\sigma = e, \mu, \tau$; per the weak interaction production and detection processes of a neutrino experiment,

$$|\sigma(\mathbf{q})\rangle = \frac{a_\sigma^\dagger(\mathbf{q})|0\rangle}{\sqrt{\langle 0|a_\sigma(\mathbf{q})a_\sigma^\dagger(\mathbf{q})|0\rangle}}, \tag{2.57}$$

and sandwich that state around Eq.(2.56). This results in a real valued

expectation value of,

$$\begin{aligned}
\langle L_\alpha^M(t) \rangle_{\sigma \rightarrow \alpha} = \sum_{k,j} \left[\text{Re} (U_{\alpha k}^* U_{\sigma k} U_{\alpha j} U_{\sigma j}^*) \right. \\
\quad \times (\cos E_k(\mathbf{q})t \cos E_j(\mathbf{q})t + v_k v_j \sin E_k(\mathbf{q})t \sin E_j(\mathbf{q})t) \\
\quad - \text{Im} (U_{\alpha k}^* U_{\sigma k} U_{\alpha j} U_{\sigma j}^*) \\
\quad \times (v_k \sin E_k(\mathbf{q})t \cos E_j(\mathbf{q})t - v_j \cos E_k(\mathbf{q})t \sin E_j(\mathbf{q})t) \\
\quad \left. - \text{Re} (U_{\alpha k}^* U_{\sigma k}^* U_{\alpha j} U_{\sigma j}) \sqrt{1 - v_k^2} \sqrt{1 - v_j^2} \sin E_k(\mathbf{q})t \sin E_j(\mathbf{q})t \right], \tag{2.58}
\end{aligned}$$

where $\langle L_\alpha^M(t) \rangle_{\sigma \rightarrow \alpha}$ denotes $\langle \sigma(\mathbf{q}) | L_\alpha^M(t) | \sigma(\mathbf{q}) \rangle$. The Majorana expectation value of Eq.(2.58) is the main result of our original work [86]. Some important features of the Majorana expectation value are,

- The cosine and sine terms are responsible for time dependent oscillations of the expectation value.
- In the last line of the equation, the quantity $\text{Re} (U_{\alpha k}^* U_{\sigma k}^* U_{\alpha j} U_{\sigma j})$ is dependent on the Majorana phases α_{21} and α_{31} . Those Majorana phases are observable CP phases and could be determined by some experiments.
- A sum over all the lepton family numbers $\sum_\alpha \langle \sigma(\mathbf{q}) | L_\alpha^M(t) | \sigma(\mathbf{q}) \rangle$ is the total lepton number. The total lepton number is not a conserved, time independent, value because of the minus sign in the last term. We will explore this further in section 3.1.
- The quantum mechanics equation for neutrino flavor oscillation Eq.(1.13) is recovered from Eq.(2.58), the Majorana expectation value, using the ultra-relativistic limit.

2.2.2 Comparison to the quantum mechanic formulation

When we take the ultra-relativistic limit of Eq.(2.58) our formulation becomes equivalent to the neutrino flavor oscillation equation derived from quantum mechanics quoted in Eq.(1.13). To prove that we start with the ultra-relativistic condition $\mathbf{q}^2 \gg m_k m_j$, which means

$E_{(k,j)}(\mathbf{q}) \approx m_{(k,j)}^2/(2|\mathbf{q}|)$. The velocities become $v_{(k,j)} \approx 1$ and $\sqrt{1 - v_{(k,j)}^2} \approx 0$ leading to,

$$\lim_{\mathbf{q}^2 \gg m_k m_j} \langle L_\alpha^M(t) \rangle_{\sigma \rightarrow \alpha} \approx \sum_{k,j} \left(\text{Re} (U_{\alpha k}^* U_{\sigma k} U_{\alpha j} U_{\sigma j}^*) \cos \frac{\Delta m_{kj}^2 t}{2|\mathbf{q}|} - \text{Im} (U_{\alpha k}^* U_{\sigma k} U_{\alpha j} U_{\sigma j}^*) \sin \frac{\Delta m_{kj}^2 t}{2|\mathbf{q}|} \right) \quad (2.59)$$

Then, we rewrite the equation with the imaginary terms,

$$\begin{aligned} \lim_{\mathbf{q}^2 \gg m_k m_j} \langle L_\alpha^M(t) \rangle_{\sigma \rightarrow \alpha} \approx \sum_{k,j} \left(\text{Re} (U_{\alpha k}^* U_{\sigma k} U_{\alpha j} U_{\sigma j}^*) \cos \frac{\Delta m_{kj}^2 t}{2|\mathbf{q}|} \right. \\ + i \text{Im} (U_{\alpha k}^* U_{\sigma k} U_{\alpha j} U_{\sigma j}^*) \cos \frac{\Delta m_{kj}^2 t}{2|\mathbf{q}|} \\ + i \text{Re} (U_{\alpha k}^* U_{\sigma k} U_{\alpha j} U_{\sigma j}^*) \sin \frac{\Delta m_{kj}^2 t}{2|\mathbf{q}|} \\ \left. + i^2 \text{Im} (U_{\alpha k}^* U_{\sigma k} U_{\alpha j} U_{\sigma j}^*) \sin \frac{\Delta m_{kj}^2 t}{2|\mathbf{q}|} \right), \end{aligned} \quad (2.60)$$

because,

$$i \sum_{k,j} \text{Im} (U_{\alpha k}^* U_{\sigma k} U_{\alpha j} U_{\sigma j}^*) \cos \frac{\Delta m_{kj}^2 t}{2|\mathbf{q}|} = 0, \quad (2.61)$$

$$i \sum_{k,j} \text{Re} (U_{\alpha k}^* U_{\sigma k} U_{\alpha j} U_{\sigma j}^*) \sin \frac{\Delta m_{kj}^2 t}{2|\mathbf{q}|} = 0, \quad (2.62)$$

$$\text{Re} (U_{\alpha k}^* U_{\sigma k} U_{\alpha j} U_{\sigma j}^*) + i \text{Im} (U_{\alpha k}^* U_{\sigma k} U_{\alpha j} U_{\sigma j}^*) = (U_{\alpha k}^* U_{\sigma k} U_{\alpha j} U_{\sigma j}^*), \quad (2.63)$$

and

$$\text{Im} (U_{\alpha k}^* U_{\sigma k} U_{\alpha j} U_{\sigma j}^*) = -\text{Im} (U_{\alpha j}^* U_{\sigma j} U_{\alpha k} U_{\sigma k}^*), \quad (2.64)$$

$$\text{Re} (U_{\alpha k}^* U_{\sigma k} U_{\alpha j} U_{\sigma j}^*) = \text{Re} (U_{\alpha j}^* U_{\sigma j} U_{\alpha k} U_{\sigma k}^*), \quad (2.65)$$

from exchange of k and j . Recall that $\Delta m_{k,j}^2 \equiv (m_k^2 - m_j^2)$ is the squared mass differences. Lastly, we use Euler's formula to find Eq.(1.13) and Eq.(2.59) match exactly,

$$\lim_{\mathbf{q}^2 \gg m_k m_j} \langle L_\alpha^M(t) \rangle_{\sigma \rightarrow \alpha} = \lim_{|\vec{p}| \gg m_{i,j}} P_{\alpha \rightarrow \beta}(t). \quad (2.66)$$

Importantly, this means our formula is more general and can be distinguished when the ultra-relativistic approximation is invalid. For example, the ultra-relativistic approximation is invalid when the momentum of the neutrinos is near or below the neutrino masses.

The quantum mechanics formula, before the ultra-relativistic approximation, was written in Eq.(1.12) with one oscillation phase $\phi_{i,j} = -(E_i(\vec{p}) - E_j(\vec{p}))t$. We rewrite Eq.(2.58) in exponential form to compare to Eq.(1.12),

$$\begin{aligned} \langle L_\alpha^M(t) \rangle_{\sigma \rightarrow \alpha} = & \frac{1}{4} \sum_{k,j} \left[U_{\alpha k}^* U_{\sigma k} U_{\alpha j} U_{\sigma j}^* \left((1 + v_k)(1 + v_j) e^{i(E_k(\mathbf{p}) - E_j(\mathbf{p}))t} \right. \right. \\ & + (1 - v_k)(1 - v_j) e^{-i(E_k(\mathbf{p}) - E_j(\mathbf{p}))t} \\ & + (1 + v_k)(1 - v_j) e^{i(E_k(\mathbf{p}) + E_j(\mathbf{p}))t} \\ & \left. \left. + (1 - v_k)(1 + v_j) e^{-i(E_k(\mathbf{p}) + E_j(\mathbf{p}))t} \right) \right. \\ & - U_{\alpha k}^* U_{\sigma k}^* U_{\alpha j} U_{\sigma j} \sqrt{1 - v_k^2} \sqrt{1 - v_j^2} \\ & \times \left(e^{i(E_k(\mathbf{p}) - E_j(\mathbf{p}))t} - e^{i(E_k(\mathbf{p}) + E_j(\mathbf{p}))t} \right) \\ & \left. + e^{-i(E_k(\mathbf{p}) - E_j(\mathbf{p}))t} - e^{-i(E_k(\mathbf{p}) + E_j(\mathbf{p}))t} \right). \quad (2.67) \end{aligned}$$

A noticeable difference between Eq.(1.12) and Eq.(2.58) is the three additional oscillation phases of,

$$\phi_{k,j}^1 = -(E_i(\mathbf{p}) - E_j(\mathbf{p}))t, \quad (2.68)$$

$$\phi_{k,j}^2 = (E_i(\mathbf{p}) + E_j(\mathbf{p}))t, \quad (2.69)$$

$$\phi_{k,j}^3 = -(E_i(\mathbf{p}) + E_j(\mathbf{p}))t. \quad (2.70)$$

All the amplitude coefficients of those phases are zero under the ultra-relativistic condition of $\mathbf{q}^2 \gg m_k m_j$ leading to $v_{k,j} \approx 1$. Which we can see by inspection,

$$(1 - v_k)(1 - v_j) \quad \text{coefficient of } \phi_{k,j}^1, \quad (2.71)$$

$$(1 + v_k)(1 - v_j) \quad \text{coefficient of } \phi_{k,j}^2, \quad (2.72)$$

$$(1 - v_k)(1 + v_j) \quad \text{coefficient of } \phi_{k,j}^3, \quad (2.73)$$

This means only the first two lines of Eq.(2.67) are non-zero, which is the same as Eq.(1.12) up to a normalization of a half. An interesting point is the frequencies induced by the new phases $\phi_{k,j}^1$, $\phi_{k,j}^2$, and $\phi_{k,j}^3$. The summed energies $E_k(\mathbf{q}) + E_j(\mathbf{q})$ will result in higher frequency oscillations compared to the subtracted energies of $E_k(\mathbf{q}) - E_j(\mathbf{q})$.

To illustrate further how our formulation is distinguishable by the additional oscillation phases we plot the momentum dependence of the absolute deviation,

$$D(\mathbf{q}) = |\langle L_\alpha^M(T) \rangle_{\sigma \rightarrow \alpha} - P_{\sigma \rightarrow \alpha}(T)|, \quad (2.74)$$

for a fixed time T in figure 2.1 from Eq.(2.58) and Eq.(1.12). We consider the lightest neutrino mass to be $m_{\text{lightest}} = 0.01\text{eV}$, which means at least one neutrino is non-relativistic when $\mathbf{q} < 0.1\text{eV}$. For the values of the mass squared differences $\Delta m_{k,j}^2$ and the PMNS matrix parameters we use the best-fit results of NuFITv5.0 [88]. Details on how the PMNS matrix is parametrized is in appendix A. Lastly, we take the Majorana phases to be zero.

In figure 2.1, for momentum below 0.1eV the absolute deviation tends to increase when approaching zero that is the effect of the additional oscillation phases $\phi_{i,j}^1$, $\phi_{i,j}^2$, and $\phi_{i,j}^3$. Additionally, below 0.01eV the absolute deviation can be greater than one. This is because the Majorana expectation value can become negative due to the last line in Eq.(2.58), which depends on the square root of $1 - v_{(k,j)}^2$.

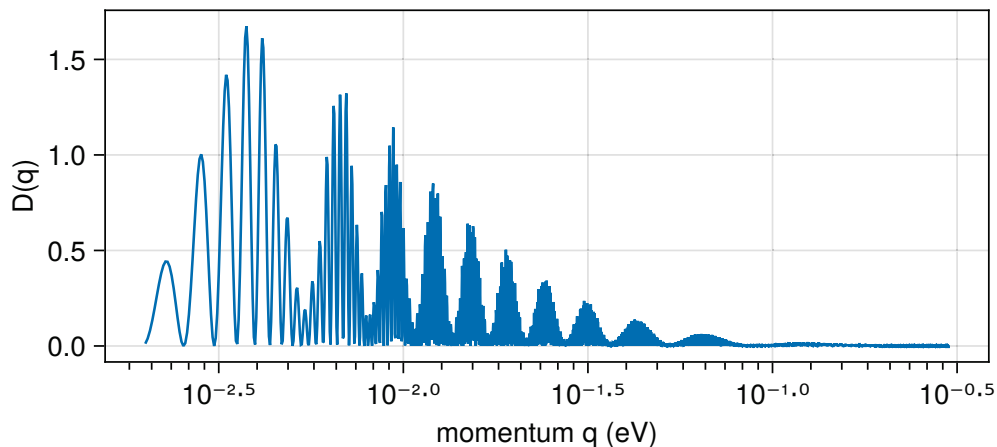


Figure 2.1: Absolute deviation between the Majorana expectation value and the quantum mechanic probability at a fixed time $T = 15\text{ps}$. We assume the lightest neutrino mass to be 0.01eV , the Majorana phases are set to zero, and all other oscillation parameters are the best-fit values from NuFITv5.0 [88]. The x-axis follows a logbase10 scaling.

For a different perspective, we plot the quantum mechanic probability Eq.(1.12) and the Majorana expectation value Eq.(2.58), separately, over a momentum interval at a fixed time T in figure 2.2. We

see the quantum mechanic probability envelopes the Majorana expectation value that is due to the common phase $\phi_{(k,j)}$. The addition phases of the Majorana expectation value, $\phi_{k,j}^1$, $\phi_{k,j}^2$, and $\phi_{k,j}^3$, cause the higher frequencies, which lead to the small scale oscillations. This effect of the addition phases holds true for appearance $e \rightarrow e$ and disappearance $e \rightarrow \mu$ transitions as illustrated in the lower and upper panels of figure 2.2.

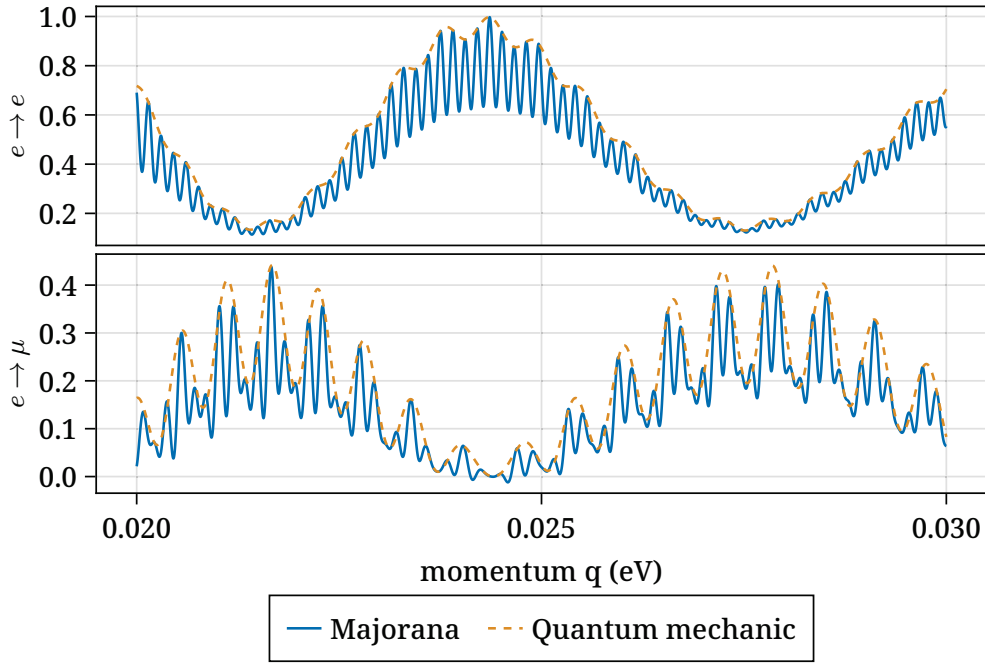


Figure 2.2: Oscillations of the Majorana expectation value overlaid with the quantum mechanic probability at a fixed time $T = 15\text{ps}$. We assume the lightest neutrino mass to be 0.01eV , and we set the Majorana phases to zero. All other oscillation parameters we use are the best-fit values from NuFITv5.0 [88].

Next we plot the appearance $e \rightarrow e$ and disappearance $e \rightarrow \mu$ transitions over a time interval for a fixed momentum of $q = 0.02\text{eV}$ in figure 2.3. We see the same higher frequencies of the Majorana expectation value being enveloped by the quantum mechanic probability. This illustrates how small scale resolution is important to distinguish our formalism.

Another distinction of our formulation, which is unrelated to the phases $\phi_{(k,j)}$, is the PMNS combination of $U_{\alpha k}^* U_{\sigma k}^* U_{\alpha j} U_{\sigma j}$. That combina-

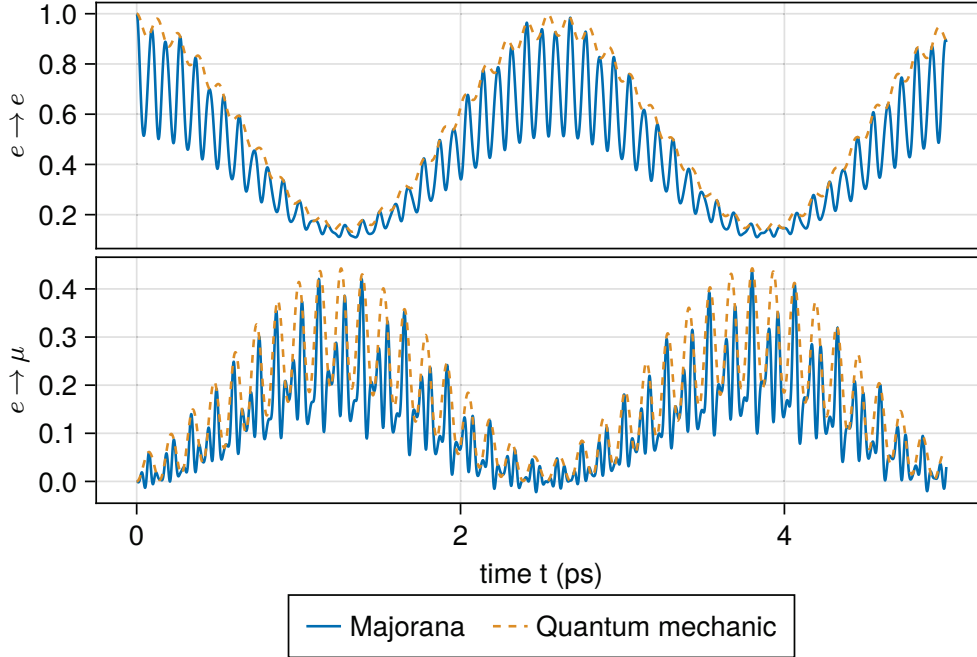


Figure 2.3: Time evolution of the Majorana expectation value overlaid with the quantum mechanics probability for a fixed momentum $\mathbf{q} = 0.02\text{eV}$. We assume the lightest neutrino mass to be 0.01eV , and we set the Majorana phases to zero. All other oscillation parameters we use are the best-fit values from NuFITv5.0 [88].

tion is unique to our Majorana expectation value and the combination depends directly on the Majorana CP phases. Importantly, that combination is suppressed by the absolute masses of the neutrinos through the term $\sqrt{1 - v_i^2} \sqrt{1 - v_j^2} = (m_i m_j) / (E_i(\mathbf{p}) E_j(\mathbf{p}))$. So, it only meaningfully contributes when the momentum is similar to, or below the absolute masses of the neutrinos. The suppression is the same reason we see greater than one values discussed before about the absolute deviation in figure 2.1.

For a final comment, the discussions of this section are also true for the external wave packet model in quantum field theory of section 1.3.4. This is because the external wave packet probability Eq.(1.31) shares the same phase, $\phi_{(k,j)}$, as the quantum mechanics probability Eq.(1.12). The external wave packet probability also has no PMNS combination of $U_{\alpha k}^* U_{\sigma k} U_{\alpha j} U_{\sigma j}$ or Majorana phase dependence.

2.3 Lepton number for Dirac neutrinos

We formulate the Dirac lepton number similarly to the Majorana lepton number of section 2.2. A major difference between the Majorana and Dirac lepton numbers is the new right-handed neutrino fields,

$$\mathcal{L}^D = \overline{\nu_{L\alpha}} i\gamma^\mu \partial_\mu \nu_{L\alpha} + \overline{\nu_{R\alpha}} i\gamma^\mu \partial_\mu \nu_{R\alpha} - \theta(t) (\overline{\nu_{R\alpha}} m_{\alpha\beta} \nu_{L\beta} + \text{h.c.}), \quad (2.75)$$

which are used to construct the mass term. The time-dependent step-function $\theta(t)$, again, guarantees an initial pure flavor state. In contrast to Eq.(2.22) of the Majorana formalism, the Dirac mass is diagonalized by two distinct unitary matrices,

$$\nu_{L\beta} = U_{\beta j} \nu_{Lj} \quad (2.76)$$

$$\nu_{R\alpha} = V_{\alpha k} \nu_{Rk} \quad (2.77)$$

$$(V^\dagger)_{k\alpha} m_{\alpha\beta} U_{\beta j} = m_k \delta_{kj}. \quad (2.78)$$

Rewriting the Lagrangian Eq.(2.75) with the four component Dirac field $\psi_k = \nu_{Rk} + \nu_{Lk}$ for a diagonal mass matrix results in the form,

$$\mathcal{L}^D = \overline{\psi}_k (i\gamma^\mu \partial_\mu - \theta(t)m_k) \psi_k. \quad (2.79)$$

In the same manner as the Majorana formalism, the step-function $\theta(t)$ separates two regions. We connect those two regions by continuity of the equation of motion for the separate fields $\nu_{L\alpha}$ and $\nu_{R\alpha}$. The zero time for the two regions is approached by reaching an infinitesimal time away,

$$\lim_{t \rightarrow 0^-} t = -\epsilon \quad \text{region one,} \quad (2.80)$$

$$\lim_{t \rightarrow 0^+} t = +\epsilon \quad \text{region two.} \quad (2.81)$$

In region one, we take the Fourier expansion of the left- and right-handed Weyl fields,

$$\nu_{L\alpha}(-\epsilon, \mathbf{x}) = \int' \frac{d^3 \mathbf{p}}{(2\pi)^3 2|\mathbf{p}|} \left(a_{L\alpha}(\mathbf{p}) u_L(\mathbf{p}) e^{i\mathbf{p}\cdot\mathbf{x}} + b_{L\alpha}^\dagger(\mathbf{p}) v_L(\mathbf{p}) e^{-i\mathbf{p}\cdot\mathbf{x}} \right) \quad (2.82)$$

$$\nu_{R\alpha}(-\epsilon, \mathbf{x}) = \int' \frac{d^3 \mathbf{p}}{(2\pi)^3 2|\mathbf{p}|} \left(a_{R\alpha}(\mathbf{p}) u_R(\mathbf{p}) e^{i\mathbf{p}\cdot\mathbf{x}} + b_{R\alpha}^\dagger(\mathbf{p}) v_R(\mathbf{p}) e^{-i\mathbf{p}\cdot\mathbf{x}} \right) \quad (2.83)$$

Recall, our integral notation \int' means the momentum regions $\{\mathbf{p} \neq 0, \mathbf{p} \in A, -\mathbf{p} \in \overline{A}\}$ with details in appendix B. We have constrained the

spinors to be normalized as,

$$u_L(\mathbf{p}) = -v_L(\mathbf{p}) = \sqrt{2|\mathbf{p}|} \begin{pmatrix} 0 \\ \phi_-(\mathbf{n}) \end{pmatrix}, \quad (2.84)$$

$$u_L(-\mathbf{p}) = -v_L(-\mathbf{p}) = i\sqrt{2|\mathbf{p}|} \begin{pmatrix} 0 \\ \phi_+(\mathbf{n}) \end{pmatrix}, \quad (2.85)$$

$$u_R(\mathbf{p}) = -v_R(\mathbf{p}) = \sqrt{2|\mathbf{p}|} \begin{pmatrix} \phi_+(\mathbf{n}) \\ 0 \end{pmatrix}, \quad (2.86)$$

$$u_R(-\mathbf{p}) = -v_R(-\mathbf{p}) = i\sqrt{2|\mathbf{p}|} \begin{pmatrix} \phi_-(\mathbf{n}) \\ 0 \end{pmatrix}. \quad (2.87)$$

Notice the imaginary unit for the negative momentum spinors appears due to Eq.(2.28) and Eq.(2.29). For convenience, we rewrite the spinor momentum dependence here,

$$\phi_+(\mathbf{n}) = \begin{pmatrix} e^{i\frac{\phi}{2}} \cos \frac{\theta}{2} \\ e^{-i\frac{\phi}{2}} \sin \frac{\theta}{2} \end{pmatrix}, \quad (2.88)$$

$$\phi_-(\mathbf{n}) = \begin{pmatrix} -e^{i\frac{\phi}{2}} \sin \frac{\theta}{2} \\ e^{-i\frac{\phi}{2}} \cos \frac{\theta}{2} \end{pmatrix}, \quad (2.89)$$

$$\phi_+(-\mathbf{n}) = \begin{pmatrix} -ie^{i\frac{\phi}{2}} \sin \frac{\theta}{2} \\ ie^{-i\frac{\phi}{2}} \cos \frac{\theta}{2} \end{pmatrix}, \quad (2.90)$$

$$\phi_-(-\mathbf{n}) = \begin{pmatrix} ie^{i\frac{\phi}{2}} \cos \frac{\theta}{2} \\ ie^{-i\frac{\phi}{2}} \sin \frac{\theta}{2} \end{pmatrix}. \quad (2.91)$$

In addition, the operators after the expansion obey the usual anti-commutation relations,

$$\left. \begin{aligned} \{a_{L\alpha}(\mathbf{p}), a_{L\beta}^\dagger(\mathbf{q})\} \\ \{b_{L\alpha}(\mathbf{p}), b_{L\beta}^\dagger(\mathbf{q})\} \end{aligned} \right\} = 2|\mathbf{p}|(2\pi)^3 \delta^{(3)}(\mathbf{p} - \mathbf{q}) \delta_{\alpha\beta}, \quad (2.92)$$

with all others being zero.

In region two, we use the on-shell Fourier expansion on the Dirac field $\psi_i(+\epsilon, \mathbf{x})$ from Eq.(2.79),

$$\begin{aligned} \psi_k(+\epsilon, \mathbf{x}) = \int' \frac{d^3\mathbf{p}}{(2\pi)^3 2E_k(\mathbf{p})} \sum_h \left(a_k(\mathbf{p}, h) u_k(\mathbf{p}, h) e^{i\mathbf{p}\cdot\mathbf{x}} \right. \\ \left. + b_k^\dagger(\mathbf{p}, h) v_k(\mathbf{p}, h) e^{-i\mathbf{p}\cdot\mathbf{x}} \right), \end{aligned} \quad (2.93)$$

where h denotes the spinor helicity and $E_k^2(\mathbf{p}) = |\mathbf{p}|^2 + m_k^2$ is the energy of the mass states. The spinors are normalized the same as Eq.(2.37) though Eq.(2.40) and obey the same orthogonality, completeness relations. Lastly, the operators obey the usual anti-commutation relations,

$$\{a_k(\mathbf{p}, h), a_j^\dagger(\mathbf{q}, h)\} = \{b_k(\mathbf{p}, h), b_j^\dagger(\mathbf{q}, h)\} = 2E_k(\mathbf{p})(2\pi)^3 \delta^{(3)}(\mathbf{p} - \mathbf{q}) \delta_{kj}, \quad (2.94)$$

and all others are zero. The operators $a_k(\mathbf{p}, h)$ and $b_k(\mathbf{p}, h)$ are distinct from the creation and annihilation operators of Eq.(2.92). Then, we use the continuity of the equation of motion, discussed in appendix B, to find two connections between the Fourier expanded fields,

$$\lim_{\epsilon \rightarrow 0^+} \nu_{Lk}(+\epsilon, \mathbf{x}) = \lim_{\epsilon \rightarrow 0^+} \sum_{\alpha} U_{\alpha k}^* \nu_{L\alpha}(-\epsilon, \mathbf{x}), \quad (2.95)$$

$$\lim_{\epsilon \rightarrow 0^+} \nu_{Rk}(+\epsilon, \mathbf{x}) = \lim_{\epsilon \rightarrow 0^+} \sum_{\beta} V_{\beta k}^* \nu_{R\beta}(-\epsilon, \mathbf{x}). \quad (2.96)$$

We use the connections of Eq.(2.95) and Eq.(2.96) to derive relations between the operators of Eq.(2.82), Eq.(2.83), and Eq.(2.93). After we split the momentum regions to be $\{\mathbf{p} \neq 0, \mathbf{p} \in A, -\mathbf{p} \in \bar{A}\}$ the operator connections are,

$$a_{L\alpha}(\pm\mathbf{p}) = \sum_k^3 U_{\alpha k} \frac{\sqrt{N_k(\mathbf{p})2|\mathbf{p}|}}{2E_k(\mathbf{p})} \left(a_k(\pm\mathbf{p}, -) + i \frac{m_k}{N_k} b_k^\dagger(\mp\mathbf{p}, -) \right), \quad (2.97)$$

$$b_{L\alpha}^\dagger(\pm\mathbf{p}) = \sum_k^3 U_{\alpha k} \frac{\sqrt{N_k(\mathbf{p})2|\mathbf{p}|}}{2E_k(\mathbf{p})} \left(b_k^\dagger(\pm\mathbf{p}, +) - i \frac{m_k}{N_k} a_k(\mp\mathbf{p}, +) \right), \quad (2.98)$$

$$a_{R\alpha}(\pm\mathbf{p}) = \sum_j^3 V_{\alpha j} \frac{\sqrt{N_j(\mathbf{p})2|\mathbf{p}|}}{2E_j(\mathbf{p})} \left(a_j(\pm\mathbf{p}, +) + i \frac{m_j}{N_j} b_j^\dagger(\mp\mathbf{p}, +) \right), \quad (2.99)$$

$$b_{R\alpha}^\dagger(\pm\mathbf{p}) = \sum_j^3 V_{\alpha j} \frac{\sqrt{N_j(\mathbf{p})2|\mathbf{p}|}}{2E_j(\mathbf{p})} \left(b_j^\dagger(\pm\mathbf{p}, -) - i \frac{m_j}{N_j} a_j(\mp\mathbf{p}, -) \right). \quad (2.100)$$

Notice the two differences between the left-handed $a_{L\alpha}(\pm\mathbf{p})$ and the right-handed $a_{R\alpha}(\pm\mathbf{p})$ versions are,

1. the exchange of the mixing matrices $U_{\alpha k} \leftrightarrow V_{\alpha j}$,
2. and the exchange of the massive operator helicities $a_k(\pm\mathbf{p}, h) \leftrightarrow a_k(\pm\mathbf{p}, -h)$ and $b_k^\dagger(\pm\mathbf{p}, h) \leftrightarrow b_k^\dagger(\pm\mathbf{p}, -h)$.

Similar to the Majorana relations of Eq.(2.46) and Eq.(2.47), there is a non-trivial mixing between the Dirac operators $a_k(\pm\mathbf{p}, h)$ and the Weyl operators $a_{L\alpha}(\pm\mathbf{p})$. The time evolution form of the operators are solved by writing Eq.(2.93) as $\psi_k(t, \mathbf{x})$, which means the operators are multiplied by,

$$a_k(\mathbf{p}, h) \rightarrow a_k(\mathbf{p}, h)e^{-iE_k(\mathbf{p})t}, \quad (2.101)$$

$$b_k^\dagger(\mathbf{p}, h) \rightarrow b_k^\dagger(\mathbf{p}, h)e^{iE_k(\mathbf{p})t}. \quad (2.102)$$

Then the equations Eq.(2.97) though Eq.(2.100) become time dependent,

$$a_{L\alpha}(\pm\mathbf{p}, t) = \sum_k^3 U_{\alpha k} \frac{\sqrt{N_k(\mathbf{p})2|\mathbf{p}|}}{2E_k(\mathbf{p})} \left(a_k(\pm\mathbf{p}, -)e^{-iE_k(\mathbf{p})t} + i\frac{m_k}{N_k} b_k^\dagger(\mp\mathbf{p}, -)e^{iE_k(\mathbf{p})t} \right), \quad (2.103)$$

$$b_{L\alpha}^\dagger(\pm\mathbf{p}, t) = \sum_k^3 U_{\alpha k} \frac{\sqrt{N_k(\mathbf{p})2|\mathbf{p}|}}{2E_k(\mathbf{p})} \left(b_k^\dagger(\pm\mathbf{p}, +)e^{iE_k(\mathbf{p})t} - i\frac{m_k}{N_k} a_k(\mp\mathbf{p}, +)e^{-iE_k(\mathbf{p})t} \right), \quad (2.104)$$

$$a_{R\alpha}(\pm\mathbf{p}, t) = \sum_j^3 V_{\alpha j} \frac{\sqrt{N_j(\mathbf{p})2|\mathbf{p}|}}{2E_j(\mathbf{p})} \left(a_j(\pm\mathbf{p}, +)e^{-iE_j(\mathbf{p})t} + i\frac{m_j}{N_j} b_j^\dagger(\mp\mathbf{p}, +)e^{iE_j(\mathbf{p})t} \right), \quad (2.105)$$

$$b_{R\alpha}^\dagger(\pm\mathbf{p}, t) = \sum_j^3 V_{\alpha j} \frac{\sqrt{N_j(\mathbf{p})2|\mathbf{p}|}}{2E_j(\mathbf{p})} \left(b_j^\dagger(\pm\mathbf{p}, -)e^{iE_j(\mathbf{p})t} - i\frac{m_j}{N_j} a_j(\mp\mathbf{p}, -)e^{-iE_j(\mathbf{p})t} \right). \quad (2.106)$$

We desire to write the time evolution solely in terms of the Weyl operators $a_{L\alpha}(\pm\mathbf{p})$, $a_{R\alpha}(\pm\mathbf{p})$, $b_{L\alpha}^\dagger(\pm\mathbf{p})$, $b_{R\alpha}^\dagger(\pm\mathbf{p})$. To accomplish that we will substitute for the Dirac operators $a_k(\pm\mathbf{p}, h)$ and $b_k^\dagger(\mp\mathbf{p}, h)$ from Eq.(2.97) though (2.100), which we derived from the continuity condition. Then

we expand the exponential into sine and cosine components to find,

$$a_{L\alpha}(\pm\mathbf{p}, t) = \sum_{\beta=e}^{\tau} \sum_k \left[U_{\alpha k} U_{\beta k}^* (\cos E_k(\mathbf{p})t - i v_k \sin E_k(\mathbf{p})t) a_{L\beta}(\pm\mathbf{p}) \right. \\ \left. \mp U_{\alpha k} V_{\beta k}^* \sqrt{1 - v_k^2} \sin E_k(\mathbf{p})t b_{R\beta}^\dagger(\mp\mathbf{p}) \right], \quad (2.107)$$

$$a_{L\alpha}^\dagger(\pm\mathbf{p}, t) = \sum_{\gamma=e}^{\tau} \sum_k \left[U_{\alpha k}^* U_{\gamma k} (\cos E_k(\mathbf{p})t + i v_k \sin E_k(\mathbf{p})t) a_{L\gamma}^\dagger(\pm\mathbf{p}) \right. \\ \left. \mp U_{\alpha k}^* V_{\beta k} \sqrt{1 - v_k^2} \sin E_k(\mathbf{p})t b_{R\gamma}(\mp\mathbf{p}) \right], \quad (2.108)$$

$$b_{L\alpha}(\pm\mathbf{p}, t) = \sum_{\beta=e}^{\tau} \sum_k \left[U_{\alpha i}^* U_{\beta k} (\cos E_k(\mathbf{p})t - i v_k \sin E_k(\mathbf{p})t) b_{L\beta}(\pm\mathbf{p}) \right. \\ \left. \mp U_{\alpha k}^* V_{\beta k} \sqrt{1 - v_k^2} \sin E_k(\mathbf{p})t a_{R\beta}^\dagger(\mp\mathbf{p}) \right], \quad (2.109)$$

$$b_{L\alpha}^\dagger(\pm\mathbf{p}, t) = \sum_{\gamma=e}^{\tau} \sum_k \left[U_{\alpha k} U_{\gamma k}^* (\cos E_k(\mathbf{p})t + i v_k \sin E_k(\mathbf{p})t) b_{L\gamma}^\dagger(\pm\mathbf{p}) \right. \\ \left. \mp U_{\alpha k} V_{\beta k}^* \sqrt{1 - v_k^2} \sin E_k(\mathbf{p})t a_{R\gamma}(\mp\mathbf{p}) \right], \quad (2.110)$$

where $v_k = |\mathbf{p}|/E_k(\mathbf{p})$ and $\sqrt{1 - v_k^2} = m_k/E_k(\mathbf{p})$. Using our knowledge from Eq.(2.97) through Eq.(2.100), we can identify the right-handed versions of Eq.(2.107) through Eq.(2.110) the time evolution operators from,

1. replacements of the mixing matrices $U_{(\alpha,\beta,\gamma)k} \leftrightarrow V_{(\alpha,\beta,\gamma)k}$,
2. swapping of the operator handedness $a_{R(\beta,\gamma)}(\pm\mathbf{p}) \leftrightarrow a_{L(\beta,\gamma)}(\pm\mathbf{p})$ and $b_{R(\beta,\gamma)}(\pm\mathbf{p}) \leftrightarrow b_{L(\beta,\gamma)}(\pm\mathbf{p})$.

We emphasize the time dependent operators will lead to phenomena equivalent to neutrino oscillations, because of the non-trivial mixing of the operators. For example, the time evolution of the operator $a_{L\alpha}(t, \pm\mathbf{p})$ depends on the creation operator $b_{R\beta}^\dagger(\mp\mathbf{p})$ and the annihilation operator $a_{L\beta}(\pm\mathbf{p})$. Naively, one may expect only a dependence on the annihilation operator $a_{L\beta}(\pm\mathbf{p})$. In the next subsection we will derive how the non-trivial mixing leads to phenomena similar to neutrino oscillations.

2.3.1 Time evolution of Dirac family numbers

For the Dirac formulation we have two types of lepton family Heisenberg operators, which we denote $L_\alpha^L(t)$ and $L_\alpha^R(t)$. The summation of those two operators is what we assign the lepton family numbers to based on the charged lepton in the $SU(2)_L$ doublet from the weak interaction L_e, L_μ, L_τ . The two lepton family numbers are then,

$$L_\alpha^L(t) = \int d^3x : \overline{\nu_{L\alpha}}(t, \mathbf{x}) \gamma^0 \nu_{L\alpha}(t, \mathbf{x}) :, \quad (2.111)$$

$$L_\alpha^R(t) = \int d^3x : \overline{\nu_{R\alpha}}(t, \mathbf{x}) \gamma^0 \nu_{R\alpha}(t, \mathbf{x}) :, \quad (2.112)$$

and

$$L_\alpha^D(t) = L_\alpha^L(t) + L_\alpha^R(t). \quad (2.113)$$

The notation $::$ denotes normal ordering according to the $a_{(L,R)\alpha}(\pm\mathbf{p})$ and $b_{(L,R)\alpha}(\pm\mathbf{p})$ vacuum. First, we focus on the operator of left-handed lepton family number L_α^L by substituting the time dependent form of Eq.(2.82). The substitutions hold the two regions for \mathbf{p} ,

$$L_\alpha^L(t) = \int_{\mathbf{p} \in A} \frac{d\mathbf{p}}{(2\pi)^3 2|\mathbf{p}|} \left(a_{L\alpha}^\dagger(\mathbf{p}, t) a_{L\alpha}(\mathbf{p}, t) - b_{L\alpha}^\dagger(\mathbf{p}, t) b_{L\alpha}(\mathbf{p}, t) \right. \\ \left. + a_{L\alpha}^\dagger(-\mathbf{p}, t) a_{L\alpha}(-\mathbf{p}, t) - b_{L\alpha}^\dagger(-\mathbf{p}, t) b_{L\alpha}(-\mathbf{p}, t) \right). \quad (2.114)$$

Then, we substitute the time dependent operators of Eq.(2.107) through Eq.(2.110) to write the operator of the left-handed lepton family num-

ber with time independent $a_{(L,R)\alpha}(\mathbf{p})$ and $b_{(L,R)\alpha}(\mathbf{p})$;

$$\begin{aligned}
L_\alpha^L(t) = & \sum_{i,j} \sum_{\beta\gamma} \int_{p \in A} \frac{d\mathbf{p}}{(2\pi)^3 2|\mathbf{p}|} \\
& \times \left[(\cos E_i(\mathbf{p})t + iv_i \sin E_i(\mathbf{p})t) (\cos E_j(\mathbf{p})t - iv_j \sin E_j(\mathbf{p})t) \right. \\
& \times (U_{\alpha i}^* U_{\beta i} U_{\alpha j} U_{\gamma j}^* O_L^a(\mathbf{p}) - U_{\alpha i} U_{\beta i}^* U_{\alpha j}^* U_{\gamma j} O_L^b(\mathbf{p})) \\
& + \sqrt{1 - v_j^2} (\cos E_i(\mathbf{p})t \sin E_j(\mathbf{p})t + iv_i \sin E_i(\mathbf{p})t \sin E_j(\mathbf{p})t) \\
& \times (-U_{\alpha i}^* U_{\beta i} U_{\alpha j} V_{\gamma j}^* O_{LR}^{ab}(\mathbf{p}) + U_{\alpha i} U_{\beta i}^* U_{\alpha j} V_{\gamma j} O_{LR}^{ba}(\mathbf{p})) \\
& + \sqrt{1 - v_i^2} (\sin E_i(\mathbf{p})t \cos E_j(\mathbf{p})t - iv_j \sin E_i(\mathbf{p})t \sin E_j(\mathbf{p})t) \\
& \times (-U_{\alpha i}^* V_{\beta i} U_{\alpha j} U_{\gamma j}^* O_{RL}^{ab}(\mathbf{p}) + U_{\alpha i} V_{\beta i}^* U_{\alpha j}^* U_{\gamma j} O_{RL}^{ba}(\mathbf{p})) \\
& + \sqrt{1 - v_i^2} \sqrt{1 - v_j^2} \sin E_i(\mathbf{p})t \sin E_j(\mathbf{p})t \\
& \left. \times (U_{\alpha i}^* V_{\beta i} U_{\alpha j} V_{\gamma j}^* O_R^b(\mathbf{p}) - U_{\alpha i} V_{\beta i}^* U_{\alpha j}^* V_{\gamma j} O_R^a(\mathbf{p})) \right]. \tag{2.115}
\end{aligned}$$

We have compacted the operator notation to be,

$$O_L^a(\mathbf{p}) = a_{L\beta}^\dagger(\mathbf{p}) a_{L\gamma}(\mathbf{p}) + a_{L\beta}^\dagger(-\mathbf{p}) a_{L\gamma}(-\mathbf{p}), \tag{2.116}$$

$$O_L^b(\mathbf{p}) = b_{L\beta}^\dagger(\mathbf{p}) b_{L\gamma}(\mathbf{p}) + b_{L\beta}^\dagger(-\mathbf{p}) b_{L\gamma}(-\mathbf{p}), \tag{2.117}$$

$$O_R^b(\mathbf{p}) = b_{R\beta}(-\mathbf{p}) b_{R\gamma}^\dagger(-\mathbf{p}) + b_{R\beta}(\mathbf{p}) b_{R\gamma}^\dagger(\mathbf{p}), \tag{2.118}$$

$$O_R^a(\mathbf{p}) = a_{R\beta}(-\mathbf{p}) a_{R\gamma}^\dagger(-\mathbf{p}) + a_{R\beta}(\mathbf{p}) a_{R\gamma}^\dagger(\mathbf{p}), \tag{2.119}$$

for the single operators and

$$O_{LR}^{ab}(\mathbf{p}) = a_{L\beta}^\dagger(\mathbf{p}) b_{R\gamma}^\dagger(-\mathbf{p}) - a_{L\beta}^\dagger(-\mathbf{p}) b_{R\gamma}^\dagger(\mathbf{p}), \tag{2.120}$$

$$O_{LR}^{ba}(\mathbf{p}) = b_{L\beta}^\dagger(\mathbf{p}) a_{R\gamma}^\dagger(-\mathbf{p}) - b_{L\beta}^\dagger(-\mathbf{p}) a_{R\gamma}^\dagger(\mathbf{p}), \tag{2.121}$$

$$O_{RL}^{ab}(\mathbf{p}) = b_{R\beta}(-\mathbf{p}) a_{L\gamma}(\mathbf{p}) - b_{R\beta}(\mathbf{p}) a_{L\gamma}(-\mathbf{p}), \tag{2.122}$$

$$O_{RL}^{ba}(\mathbf{p}) = a_{R\beta}(-\mathbf{p}) b_{L\gamma}(\mathbf{p}) - a_{R\beta}(\mathbf{p}) b_{L\gamma}(-\mathbf{p}), \tag{2.123}$$

for the mixed operators. The right-handed lepton number $L_\alpha^R(t)$ is found by following the same replacement rules of

1. exchanging the mixing matrices $U_{(\alpha,\beta,\gamma)k} \leftrightarrow V_{(\alpha,\beta,\gamma)k}$,
2. swapping the operator handedness $a_{R(\beta,\gamma)}(\pm\mathbf{p}) \leftrightarrow a_{L(\beta,\gamma)}(\pm\mathbf{p})$ and $b_{R(\beta,\gamma)}(\pm\mathbf{p}) \leftrightarrow b_{L(\beta,\gamma)}(\pm\mathbf{p})$.

Lastly, the operator for the lepton family number in the Dirac case is $L_\alpha^D(t) = L_\alpha^L(t) + L_\alpha^R(t)$ from Eq.(2.113).

Our next step is to take the expectation value of the Dirac operator for which we prepare a normalized left-handed flavor state,

$$|\sigma_L(\mathbf{q})\rangle = \frac{a_{L\sigma}^\dagger(\mathbf{q})|0\rangle}{\sqrt{\langle 0|a_{L\sigma}(\mathbf{q})a_{L\sigma}^\dagger(\mathbf{q})|0\rangle}}, \quad (2.124)$$

which is a pure state of $\sigma_L(\mathbf{q}) = e, \mu, \tau$. That state is based on a Weak interaction production process. Then, we sandwich the state of Eq.(2.124) around Eq.(2.115) the operator of the left-handed lepton family number to get,

$$\begin{aligned} \langle L_\alpha^L(t) \rangle_{\sigma_L \rightarrow \alpha} = \sum_{i,j} \left[\text{Re} (U_{\alpha i}^* U_{\sigma i} U_{\alpha j} U_{\sigma j}^*) (\cos E_i(\mathbf{q})t \cos E_j(\mathbf{q})t \right. \\ \left. + v_i v_j \sin E_i(\mathbf{q})t \sin E_j(\mathbf{q})t \right. \\ \left. - \text{Im} (U_{\alpha i}^* U_{\sigma i} U_{\alpha j} U_{\sigma j}^*) (v_i \sin E_i(\mathbf{q})t \cos E_j(\mathbf{q})t \right. \\ \left. - v_j \sin E_j(\mathbf{q})t \cos E_i(\mathbf{q})t) \right], \end{aligned} \quad (2.125)$$

which is the left-handed expectation value, and we have used the notation $\langle L_\alpha^L(t) \rangle_{\sigma_L \rightarrow \alpha} = \langle \sigma_L(\mathbf{q}) | L_\alpha^L(t) | \sigma_L(\mathbf{q}) \rangle$. Next, we calculate the right-handed expectation value by sandwiching the state of Eq.(2.124) around the operator of the right-handed lepton family number,

$$\langle L_\alpha^R(t) \rangle_{\sigma_L \rightarrow \alpha} = \sum_{i,j} V_{\alpha i}^* U_{\sigma i} V_{\alpha j} U_{\sigma j}^* \sqrt{1 - v_i^2} \sqrt{1 - v_j^2} \sin E_i(\mathbf{p})t \sin E_j(\mathbf{p})t. \quad (2.126)$$

The sum of Eq.(2.125) and Eq.(2.126) is the Dirac expectation value,

$$\begin{aligned} \langle L_\alpha^D(t) \rangle_{\sigma_L \rightarrow \alpha} = \sum_{i,j} \left[\text{Re} (U_{\alpha i}^* U_{\sigma i} U_{\alpha j} U_{\sigma j}^*) \right. \\ \times (\cos E_i(\mathbf{q})t \cos E_j(\mathbf{q})t + v_i v_j \sin E_i(\mathbf{q})t \sin E_j(\mathbf{q})t) \\ \left. - \text{Im} (U_{\alpha i}^* U_{\sigma i} U_{\alpha j} U_{\sigma j}^*) \right. \\ \times (v_i \sin E_i(\mathbf{q})t \cos E_j(\mathbf{q})t - v_j \sin E_j(\mathbf{q})t \cos E_i(\mathbf{q})t) \\ \left. + V_{\alpha i}^* U_{\sigma i} V_{\alpha j} U_{\sigma j}^* \sqrt{1 - v_i^2} \sqrt{1 - v_j^2} \sin E_i(\mathbf{p})t \sin E_j(\mathbf{p})t \right]. \end{aligned} \quad (2.127)$$

The Dirac expectation value Eq.(2.127) is our second main result, after the Majorana expectation value Eq.(2.58), and was not featured in our original work.

Importantly, the discussion we had in section 2.2.2 about the comparison between the Majorana expectation value and quantum mechanic formulation also applies to the Dirac expectation value. Because the lines one though four match exactly between Eq.(2.58) the Majorana expectation value and Eq.(2.127) the Dirac expectation value, and the last line is suppressed by the absolute masses of the neutrinos. In the next chapter, chap.3, we will compare the Majorana and Dirac expectation values in greater detail.

Chapter 3

Comparison of Majorana and Dirac Expectation Values

The usual formulations of neutrino flavor oscillations in quantum mechanics and quantum field theory can not address the fundamental question of neutrino mass type. Being neutral fermions, the mass of neutrinos can come from three possible sources;

1. Majorana mass type,
2. Dirac mass type,
3. Majorana and Dirac mass type.

If neutrinos are Majorana fermions then the first and third mass types are possible, but if they are Dirac fermions only the second mass type is possible. High-energy experiments, in general, can not distinguish the fermion type of neutrinos¹. Kayser called this the “Practical Dirac-Majorana Confusion Theorem” [89, 90, 91, 92]. Presently, this means a different type of experiment called neutrino-less double beta decay ($0\nu\beta\beta$) is needed. However, the positive detection of neutrino-less double beta decay is only proof that neutrinos are Majorana fermions. The recent null-results of neutrino-less double beta decay experiments does not imply neutrinos are Dirac fermions[94].

Our formulation provides a look into if neutrinos are Majorana or Dirac fermions independent of neutrino-less double beta decay. This is from differences in the evolution of the expectation values Eq.(2.58)

¹Last month 05/2022, on the arXiv, it was suggested that neutrinos are Dirac fermions. Unfortunately, this is a common mistake and has been discussed by Kayser before [93].

and Eq.(2.127). We will highlight those differences in two ways, first by studying the total lepton number and second by comparing the low momentum phenomenology.

3.1 Total Lepton Number

As we introduced in section 1.1.2, total lepton number is defined as a summation over all lepton family numbers $L = L_e + L_\mu + L_\tau$. In our formulation, the total lepton number is found after taking summation over the Greek index $\alpha = e, \mu, \tau$. We take the α summation for Eq.(2.58) the Majorana expectation value and Eq.(2.127) the Dirac expectation value resulting in,

$$\sum_{\alpha} \langle \sigma(\mathbf{q}) | L_{\alpha}^M(t) | \sigma(\mathbf{q}) \rangle = 1 - 2 \sum_i |U_{\sigma i}|^2 (1 - v_i^2) \sin^2 E_i(\mathbf{q})t, \quad (3.1)$$

$$\sum_{\alpha} \langle \sigma_L(\mathbf{q}) | L_{\alpha}^D(t) | \sigma_L(\mathbf{q}) \rangle = 1, \quad (3.2)$$

where conservation of total lepton number is equal to one. The Majorana expectation value violates total lepton number as proved in Eq.(3.1) and the violation oscillates between,

$$-1 \leq \sum_i |U_{\sigma i}|^2 \frac{|\mathbf{q}|^2 - m_i^2}{|\mathbf{q}|^2 + m_i^2} \leq \sum_{\alpha} \langle \sigma(\mathbf{q}) | L_{\alpha}^M(t) | \sigma(\mathbf{q}) \rangle \leq 1. \quad (3.3)$$

From Eq.(3.2) the Dirac expectation value conserves total lepton number. The Dirac lepton family number oscillations are bounded by

$$0 \leq \langle \sigma_L(\mathbf{q}) | L_{\alpha}^D(t) | \sigma_L(\mathbf{q}) \rangle \leq 1. \quad (3.4)$$

The reason for the violation and conservation of the expectation values are the last terms in Eq.(2.58) and Eq.(2.127), which we reproduce in Fig.3.1 with notes. So, the reason for total lepton number violation in the Majorana expectation value is the minus sign in front of the last term. Whereas the reason for conservation in the Dirac expectation value is the plus sign. Unsurprisingly, based on our discussion at the beginning of chapter 2, both of those terms are directly proportional to the absolute masses of the neutrinos. As an example, we outline the taking a sum over α for the Dirac expectation value. We start with separating the expectation according to Eq.(2.113) into

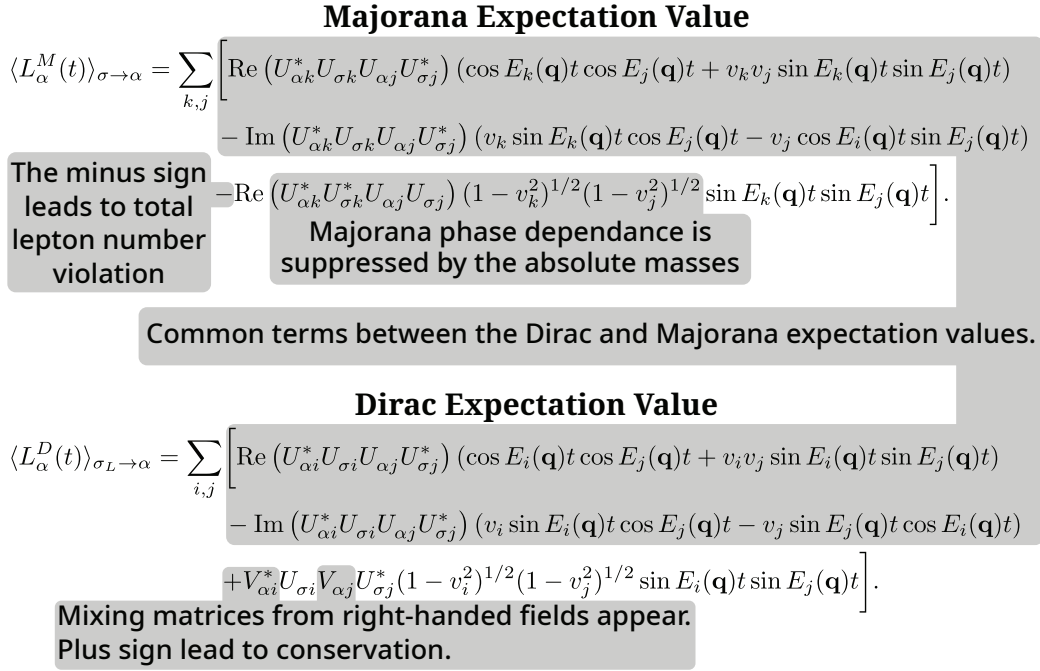


Figure 3.1: Comparison of the Majorana and Dirac expectation values.

Eq.(2.125) the left-handed and Eq.(2.126) the right-handed expectation values. Next, we separately sum over α to find the total lepton numbers,

$$\sum_{\alpha} \langle L_\alpha^L(t) \rangle_{\sigma_L \rightarrow \alpha} = \sum_i |U_{\sigma i}|^2 (\cos^2 E_i(\mathbf{q})t + v_i^2 \sin^2 E_i(\mathbf{q})t), \quad (3.5)$$

$$\sum_{\alpha} \langle L_\alpha^R(t) \rangle_{\sigma_L \rightarrow \alpha} = \sum_i |U_{\sigma i}|^2 (1 - v_i^2) \sin^2 E_i(\mathbf{p})t. \quad (3.6)$$

When we recover the Dirac expectation value as the summation of Eq.(3.5) and Eq.(3.6) the sine squared terms with the coefficient v_i^2 cancel. Then, the cosine squared plus sine squared is equal to one and the sum over the PMNS matrices squared is also one. The summation of α for the Majorana expectation value has a term similar to Eq.(3.6) expect the Majorana case has an overall minus sign. That is the minus sign, which leads to total lepton number violation.

Because the effect of the conservation or violation terms is suppressed by the masses of the neutrinos though $\sqrt{1 - v_i^2} = m_i / (E_i(\mathbf{q}))$, for larger momenta differences between the Majorana and Dirac expectation values is negligible. We illustrate this with figure 3.2, where we consider the lightest neutrino mass to be $m_{\text{lightest}} = 0.01\text{eV}$, which

means at least one neutrino is non-relativistic when $q < 0.1\text{eV}$. Similar to chapter 2, the values of the mass squared differences $\Delta m_{i,j}^2$ and the PMNS matrix parameters² are the best-fit results of NuFITv5.0 [88]. Lastly, we take the Majorana phases to be zero. In figure 3.2 the Majorana expectation value starts to take negative values below $q = 0.01\text{eV}$, whereas the Dirac expectation value is always positive. Additionally, the negative values are larger as the momentum moves toward zero.

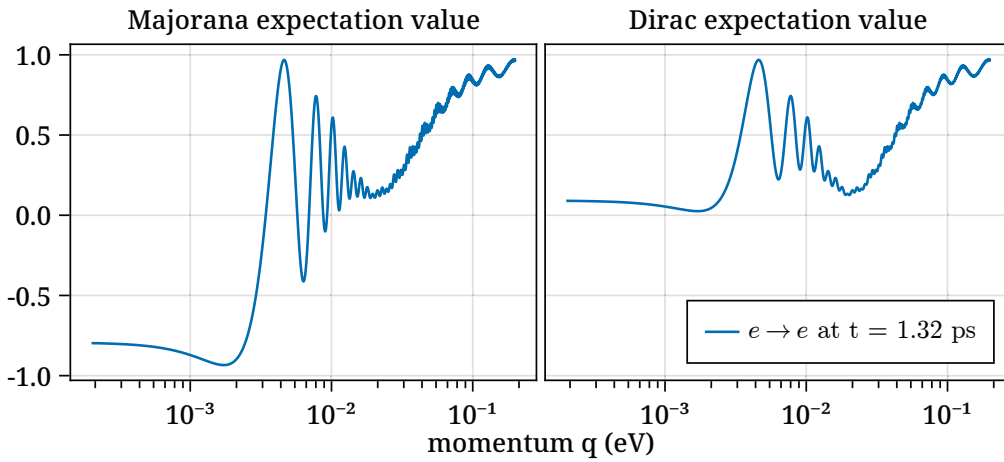


Figure 3.2: Comparison of the Majorana and Dirac expectation values at a fixed time. We set the Majorana phases to zero and assume the lightest neutrino mass to be 0.01eV . All other oscillation parameters we use are the best-fit values from NuFITv5.0 [88]. The x-axis is a logbase10 scale.

We also illustrate with figure 3.3 how the different appearance $\sigma \rightarrow \alpha$ and disappearance $\sigma \rightarrow \sigma$ Majorana expectation values are unequally affected by the lepton number violation. In the left panel for momentum $q = 0.0002\text{eV}$ the $e \rightarrow e$ disappearance oscillates to larger negative values than the $e \rightarrow \mu$ and $e \rightarrow \tau$ appearance expectation values, although all three expectation values do oscillate to negative amplitudes. Comparing the two panels we see at a larger momentum of $q = 0.2\text{eV}$ the three expectation values do not take on negative amplitudes. Thus, the Majorana and Dirac expectation values are indistinguishable.

It is important to notice the x-axis timescale is different among the

²Details on how the PMNS matrix is parametrized is in appendix A.

panels of figure 3.3. For the larger momentum of $q = 0.2\text{eV}$ we have taken a longer timescale, than the momentum of $q = 0.0002$. We have changed the timescale because the higher frequency phases $\phi_{k,j}^1$, $\phi_{k,j}^2$, and $\phi_{k,j}^3$ we discussed in section 2.2.2 dominate the amplitude for the smaller momentum $q = 0.0002\text{eV}$.

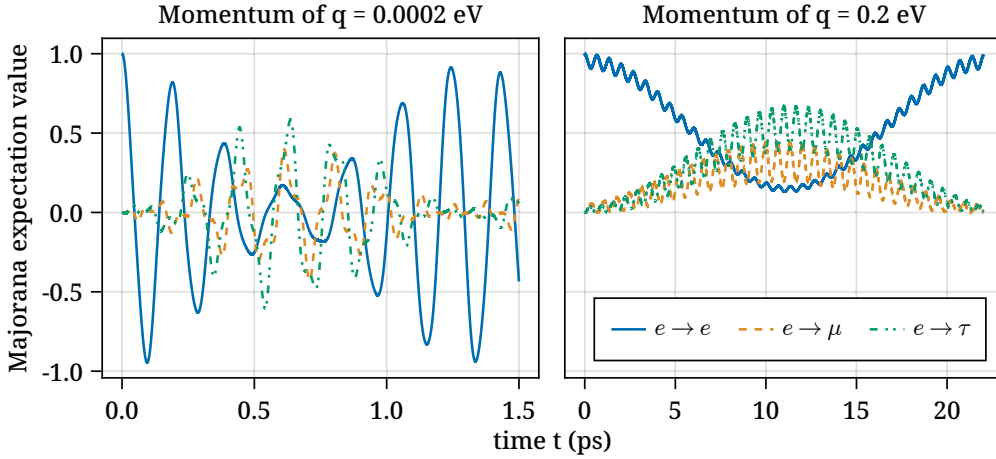


Figure 3.3: Comparison of the Majorana expectation values at different fixed momenta over time. We use the best-fit oscillation parameters from NuFITv5.0 [88], assume the lightest neutrino mass to be 0.01eV , and set the Majorana phases to zero.

3.2 Phenomenology of the lepton family numbers

We focus on the interesting phenomenology that occurs for the expectation values of the three lepton family numbers $\alpha = e, \mu, \tau$. First, phenomenology of Eq.(2.127) the Dirac expectation value depends strongly on the model that generates the Dirac mass term for the neutrinos. This is because the mixing matrix related to the right-handed field $V_{\alpha k}$ is ill-defined, unless we consider the model that generates the Dirac neutrino mass term. In this section, for generality, we treat the influence of the mixing matrix $V_{\alpha k}$ as a missing component for the total lepton number. This results in an equation similar to Eq.(3.5);

$$\sum_{\alpha} \langle L_{\alpha}^L(t) \rangle_{\sigma_L \rightarrow \alpha} = 1 - \sum_k |U_{\sigma k}|^2 (1 - v_k^2) \sin^2 E_k(\mathbf{q})t, \quad (3.7)$$

recall our notation $\langle L_\alpha^L(t) \rangle_{\sigma_L \rightarrow \alpha} = \langle \sigma_L(\mathbf{q}) | L_\alpha^L(t) | \sigma_L(\mathbf{q}) \rangle$. This means we are only considering the phenomenology of Eq.(2.125) the left-handed expectation value. An interesting part of Eq.(2.125) is the influence of the summed energy phases,

$$\phi_{i,j}^2 = (E_i(\mathbf{p}) + E_j(\mathbf{p})) t, \quad (3.8)$$

$$\phi_{i,j}^3 = - (E_i(\mathbf{p}) + E_j(\mathbf{p})) t, \quad (3.9)$$

at different momenta. We already discussed how those phases can be used to distinguish our formulation from the quantum mechanic probability in Section 2.2.2, but we have not discussed how we can use them to help distinguish the neutrino mass hierarchy.

The neutrino mass hierarchy is an open question about if the mass eigenstate ν_3 is the heaviest or the lightest in standard neutrino oscillations as introduced in section 1.4. Commonly in this is called the normal (ν_3 is the heaviest) or inverted (ν_3 is the lightest) hierarchy problem. Near future neutrino experiments are expected to answer that question, but they require a high degree of precision and a large amount of statistics. This is because the oscillation phase the experiments are sensitive to, $\phi_{i,j} = (E_i(\mathbf{p}) - E_j(\mathbf{p})) t$, is only weakly related to the mass hierarchy. The additional phases $\phi_{i,j}^2$ and $\phi_{i,j}^3$ of our formulation have a stronger relation to the mass hierarchy and become more pronounced at lower momenta. We illustrate the differences of the left-handed expectation and the quantum mechanic probability in figure 3.4. We can clearly see the influence of the high frequency oscillations in the left-handed expectation value for the inverted hierarchy. Furthermore, as the momentum approaches zero the amplitude of the high frequency oscillations increases.

For the time evolution, the additional phases appear as high frequencies within the envelope of the oscillations. As we lower the momentum the amplitude of the additional phases increases, changing the effects of constructive and destructive interference. This effect is clear if we rewrite Eq.(2.125) from trig products to sums,

$$\begin{aligned} \langle L_\alpha^D(t) \rangle_{\sigma_L \rightarrow \alpha} = \frac{1}{2} \sum_{i,j} & \left[\text{Re} (U_{\alpha i}^* U_{\sigma i} U_{\alpha j} U_{\sigma j}^*) \{ (1 + v_i v_j) \cos[(E_i(\mathbf{q}) - E_j(\mathbf{q}))t] \right. \\ & \quad \left. + (1 - v_i v_j) \cos[(E_i(\mathbf{q}) + E_j(\mathbf{q}))t] \right] \\ & - \text{Im} (U_{\alpha i}^* U_{\sigma i} U_{\alpha j} U_{\sigma j}^*) \{ (v_i - v_j) \sin[(E_i(\mathbf{q}) + E_j(\mathbf{q}))t] \\ & \quad \left. + (v_i + v_j) \sin[E_i(\mathbf{q}) - E_j(\mathbf{q})t] \} \right]. \end{aligned} \quad (3.10)$$

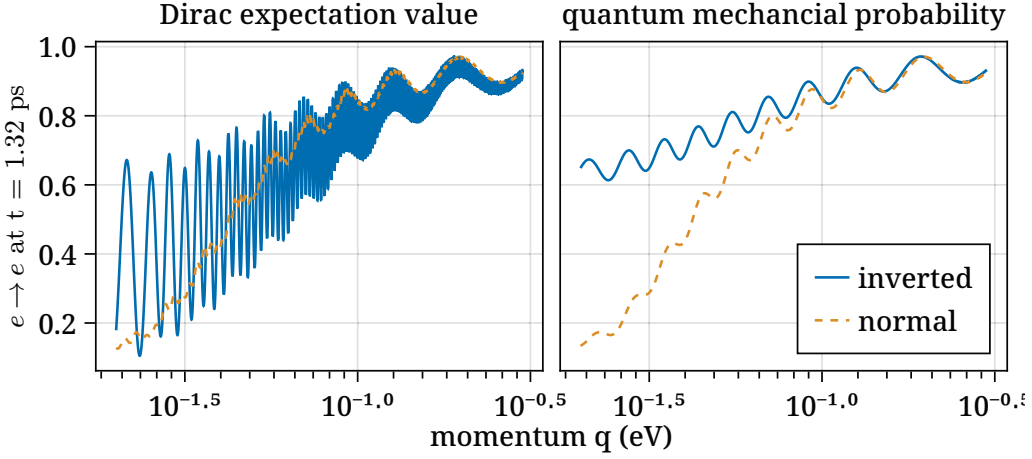


Figure 3.4: Comparison of the Dirac expectation value for inverted mass hierarchy and normal mass hierarchy at different momenta. We use the best-fit oscillation parameters from NuFITv5.0 [88] and assume the lightest neutrino mass to be 0.01eV. The x-axis uses a log base 10 scale.

Recall that $v_i = |\mathbf{q}|/(E_i(\mathbf{q}))$, which means for smaller momentum compared to the neutrino masses, v_i is smaller from one. So the terms

$$(1 - v_i v_j) \cos[(E_i(\mathbf{q}) + E_j(\mathbf{q}))t], \quad (3.11)$$

$$(v_i - v_j) \sin[(E_i(\mathbf{q}) + E_j(\mathbf{q}))t], \quad (3.12)$$

from Eq.(3.10) become more important to the oscillation amplitude for smaller momenta. This allows our formulation to have a greater distinction in the neutrino mass hierarchies at smaller momenta. We illustrate this effect over a wide momenta range in figure 3.5. Clearly, the higher frequency oscillations have a greater influence on the amplitude of the left-handed expectation value as momentum decreases. Furthermore, the higher frequencies are more pronounced in the inverted hierarchy case. We understand this by considering the effect of the mass hierarchy on the summed energy phases $(E_i(\mathbf{q}) + E_j(\mathbf{q}))t$. For the inverted hierarchy two heavy states exist, ν_1 and ν_2 that generate the frequencies,

$$f_{22}(\mathbf{q}) = E_2(\mathbf{q}) + E_2(\mathbf{q}) \quad \text{the highest frequency,} \quad (3.13)$$

$$f_{21}(\mathbf{q}) = E_2(\mathbf{q}) + E_1(\mathbf{q}), \quad (3.14)$$

$$f_{11}(\mathbf{q}) = E_1(\mathbf{q}) + E_1(\mathbf{q}), \quad (3.15)$$

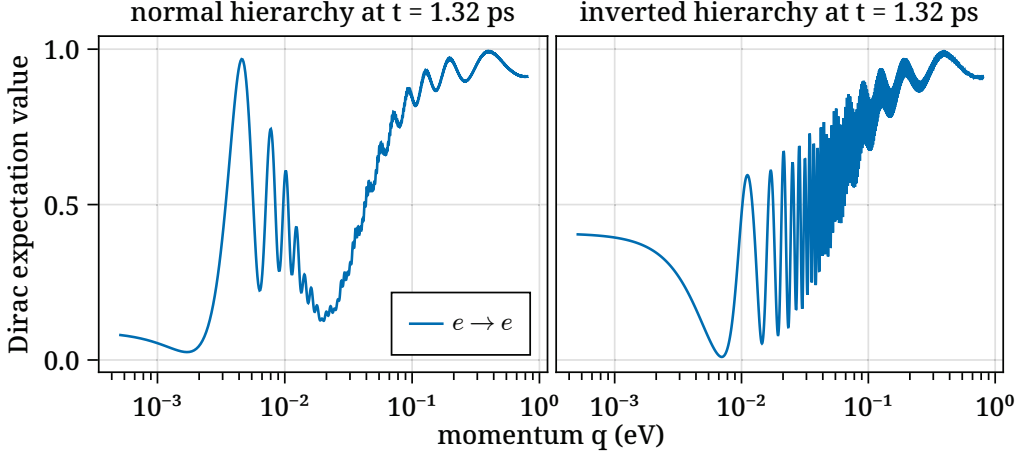


Figure 3.5: Comparison of the Dirac expectation value for inverted mass hierarchy and normal mass hierarchy at different momenta. We use the best-fit oscillation parameters from NuFITv5.0 [88] and assume the lightest neutrino mass to be 0.01eV. The x-axis uses a log base 10 scale.

because the mass squared difference of $\Delta m_{21}^2 = 7.25 \times 10^{-5} \text{ eV}^2$ is two orders of magnitude smaller than $|\Delta m_{31}^2| = 2.498 \times 10^{-3} \text{ eV}^2$. In the normal hierarchy only one heavy state exists, ν_3 , so we are left with a single high frequency and some medium frequencies,

$$f_{33}(\mathbf{q}) = E_3(\mathbf{q}) + E_3(\mathbf{q}) \quad \text{the high frequency,} \quad (3.16)$$

$$f_{31}(\mathbf{q}) = E_3(\mathbf{q}) + E_1(\mathbf{q}) \quad \text{a medium frequency,} \quad (3.17)$$

$$f_{23}(\mathbf{q}) = E_2(\mathbf{q}) + E_3(\mathbf{q}) \quad \text{a medium frequency,} \quad (3.18)$$

and the mass squared difference becomes $|\Delta m_{32}^2| = 2.517 \times 10^{-3} \text{ eV}^2$. In summary, our formulation has a stronger relation to the neutrino mass hierarchy and the strength becomes more pronounced at lower momenta, because of the additional phases $\phi_{i,j}^2$ and $\phi_{i,j}^3$.

For Eq.(2.58) the Majorana expectation value, the exact Majorana mass model is not important to the general phenomenology. This is because the Majorana phases are physical parameters that can in principle take on any value, see the discussion in appendix A. In our formulation the PMNS term $\text{Re}(U_{\alpha k}^* U_{\sigma k} U_{\alpha j} U_{\sigma j})$ is directly proportional to the Majorana phases α_{21} and α_{31} . That term only has significance for lower momentum, as we have noted at the end of section 2.2 after Eq.(2.58); and in the middle of section 3.1. We illustrate the effect of

the Majorana phases in figure 3.6 by considering the cases they have the least and the greatest contributions to the Majorana expectation value,

$$(\alpha_{21}, \alpha_{31}) = (0, 2\delta) \quad \text{the least effect,} \quad (3.19)$$

$$(\alpha_{21}, \alpha_{31}) = (\pi, \pi + 2\delta) \quad \text{the greatest effect.} \quad (3.20)$$

In the left panel of figure 3.6 the Majorana phases are chosen to be

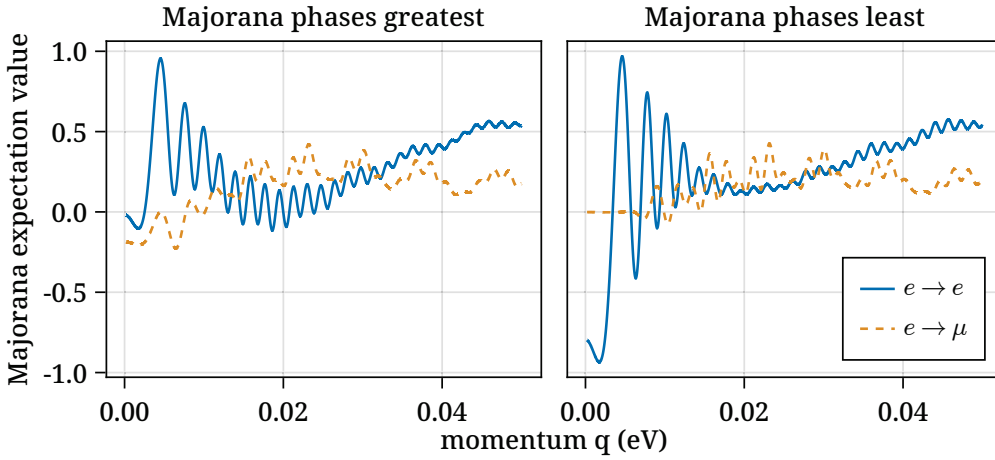


Figure 3.6: Comparison of different Majorana phases over a momenta range. We use the best-fit oscillation parameters from NuFITv5.0 [88], assume the lightest neutrino mass to be 0.01eV, and use normal hierarchy.

their greatest values. Near the momentum $q = 0.02\text{eV}$ the disappearance amplitude $e \rightarrow e$ for the Majorana expectation value becomes negative. Contrast this to the right panel where the Majorana phases are their least values and the disappearance amplitude is positive near the momentum $q = 0.02\text{eV}$. Additionally, for momenta closer to zero the Majorana phases at their least values do not constrain the negative disappearance amplitude. However, when the Majorana phases are at their greatest values the disappearance amplitude is almost always positive. This illustrates how the PMNS term $\text{Re}(U_{\alpha k}^* U_{\sigma k}^* U_{\alpha j} U_{\sigma j})$ and the Majorana phases are suppressed by the masses of the neutrinos through $\sqrt{1 - v_{(k,j)}^2} = m_{(k,j)}/(E_{(k,j)}(q))$ in Eq.(2.58).

3.3 Summary

From this chapter we have illustrated how our formulation provides a look into if neutrinos are Majorana or Dirac fermions. We have done this by investigating from differences in the evolution of the expectation values Eq.(2.58) and Eq.(2.127). We have investigated those differences in two ways, first by studying the total lepton number and second by comparing the low momentum phenomenology. For total lepton number, we found for the Dirac expectation value the total lepton number is always conserved and for the Majorana expectation value violates total lepton number. We highlighted how this occurs though figure 3.1 and illustrated the effect on disappearance and appearance calculations in figures 3.2 and 3.3. For the low momentum phenomenology we discussed how our formulation has three interesting phenomenology properties,

1. we can distinguish the neutrino mass type,
2. differences from the neutrino mass hierarchy are enhanced,
3. the Majorana phases can play an important role to the Majorana Expectation value.

In the next chapter, chap. 4, we will change directions completely and discuss some theoretical implications of our formalism.

Chapter 4

Lepton number in the Schrödinger picture

For this final chapter, we will discuss the ideas from one of our other works [95]. The basis of our formulation in chapters 2 and 3 is the Heisenberg picture, where the operators of the Lepton family numbers are Heisenberg operators Eq.(2.56) and Eq.(2.113). But, in principle we can reformulate to the Schrödinger picture and reproduce the same results. We are motivated to do this because, as we stressed in chapter 2, the creation and annihilation operators of Eq.(2.46) and Eq.(2.47), Eq.(2.52) and Eq.(2.53), Eq.(2.97) through Eq.(2.100), and finally Eq.(2.107) through Eq.(2.110), have a non-trivial mixing. That suggests a non-trivial relationship between the Fock spaces of the operators.

When we do reformulate to the Schrödinger picture, we find the operator relations of Eq.(2.46) and Eq.(2.47) from the Majorana calculation can be expressed as a Bogolyubov transformation. The Bogolyubov transformation leads to a relationship between the different vacua of the operators. The Bogolyubov transformation has been applied by others to neutral particle oscillations and neutrinos as Majorana particles have been suggested to be Bogolyubov quasi-particles [78, 79, 80, 81, 82, 83, 96, 97]. To understand those ideas we will first introduce some concepts about quantum field theories that is normally not covered in high energy physics, but is discussed in condensed matter physics in section 4.1. Then, we will clarify the relationship between our original formulation in the Heisenberg picture and the other formulations in the Schrödinger picture, over sections 4.2 and 4.3.

4.1 Unitarily inequivalent representations

We set a background for the Bogolyubov transformation using a prescription of condensed matter physics [98]. We start with a many body system described by a state $|n_1, n_2, \dots\rangle$ and those states form a set $\{|n_1, n_2, \dots\rangle\}$. That set is non-countable, and can be proven for a Fermion system that uses the binary number system. For example, in a binary system the set can be written as $\{n_1 n_2 \dots n_k \dots\}$ where $n_k = 0$ or $n_k = 1$. That set is across $(0, 1)$ on the real number line and corresponds directly to the set $\{|n_1, n_2, \dots, n_k, \dots\rangle\}$. Thus, the set $\{|n_1, n_2, \dots, n_k, \dots\rangle\}$ is non-countable.

We can not use a non-countable, in other words an infinite, set for a base of a Hilbert space \mathcal{H} , which only allows countable, or finite, sets [99]. To fix this problem we can select a subset from $\{|n_1, n_2, \dots\rangle\}$ that is countable and use that subset to build the Fock space \mathcal{F} . The Fock space \mathcal{F} is a unique subspace of the Hilbert space because it holds the vacuum $|0\rangle$, or zero particle state. However, we are then faced with infinite selection of countable subsets, so an infinite number of Fock spaces \mathcal{F} , to form our Hilbert space \mathcal{H} . If we are able to define two unique subsets as the base for representing the operators $a_i, a_i^\dagger : i = 1, 2, \dots$ then those two representations form unique Fock spaces \mathcal{F} . Those Fock spaces \mathcal{F} are said to unitarily inequivalent to each other [98]. This leads to Haags theorem[100], which to simplify states;

1. when two fields are unitarily equivalent, then both are free if one is free,
2. only when the ground states are equal can their corresponding Fock spaces be unitarily equivalent.

As we introduced in section 1.3.2, neutrinos can be described by the weak states,

$$|\nu_\alpha\rangle = \sum_i U_{\alpha i}^* |\nu_i\rangle. \quad (4.1)$$

In the two flavor case the index $i = 1, 2$ tells us the flavor fields, ν_e and ν_μ , are a superposition of the massive fields ν_1 and ν_2 . So, there are two general types of Fock spaces one for the massive fields \mathcal{F}_i and the other for the flavor fields \mathcal{F}_α . Both \mathcal{F}_i and \mathcal{F}_α are unique subspaces of the Hilbert space \mathcal{H} , which means they must be treated as unitarily inequivalent. In other words, there is no unitary transformation V between the fields ν_α and ν_i that satisfies the relation,

$$\nu_\alpha = V^{-1} \nu_i V. \quad (4.2)$$

Consequently, there is also no such unitary transformation between the creation and annihilation operators of those fields.

We stressed in chapter 2, the creation and annihilation operators of Eq.(2.46) and Eq.(2.47) for the Majorana case and Eq.(2.97) through Eq.(2.100) for the Dirac case have a non-trivial mixing among themselves. That non-trivial mixing is a consequence of us creating Fock spaces \mathcal{F} in two separate regions, then connecting those regions with a continuity condition. Thus, the relations between the fields, and consequently the operators, is non-trivial because the Fock spaces are unitarily inequivalent.

As we mentioned before, each Fock space \mathcal{F} is a unique subspace due to the vacuum. In other words, the vacuum of separate Fock spaces are different and operators of one Fock space can not act upon the vacuum of a second Fock space. We will study how the unitarily inequivalence and different vacuums we use in our formalism in the next section, sec. 4.2.

4.2 The Bogolyubov transformation

For simplicity, we will only consider a single flavor case of the Majorana lepton number from section 2.1;

$$\mathcal{L}^S = i\bar{\psi}_L \gamma^\mu \partial_\mu \psi_L - \theta(t) \frac{m}{2} \left(\bar{\psi}_L^C \psi_L + \text{h.c.} \right). \quad (4.3)$$

Recall the notation of $\psi_L^C = (\psi_L)^C$ for charge conjugation. Next, we reproduce the operator relations of Eqs.(2.14) and (2.15) for convenience,

$$a(\mathbf{p}) = \frac{\sqrt{2|\mathbf{p}|N(\mathbf{p})}}{2E(\mathbf{p})} \left(a_M(\mathbf{p}, -) + \frac{im}{N(\mathbf{p})} a_M^\dagger(-\mathbf{p}, -) \right), \quad (4.4)$$

$$b(\mathbf{p}) = \frac{\sqrt{2|\mathbf{p}|N(\mathbf{p})}}{2E(\mathbf{p})} \left(a_M(\mathbf{p}, +) + \frac{im}{N(\mathbf{p})} a_M^\dagger(-\mathbf{p}, +) \right), \quad (4.5)$$

and extend them into the second momentum region of $a(-\mathbf{p})$ and $b(-\mathbf{p})$;

$$a(-\mathbf{p}) = \frac{\sqrt{2|\mathbf{p}|N(\mathbf{p})}}{2E(\mathbf{p})} \left(a_M(-\mathbf{p}, -) - \frac{im}{N(\mathbf{p})} a_M^\dagger(\mathbf{p}, -) \right), \quad (4.6)$$

$$b(-\mathbf{p}) = \frac{\sqrt{2|\mathbf{p}|N(\mathbf{p})}}{2E(\mathbf{p})} \left(a_M(-\mathbf{p}, +) - \frac{im}{N(\mathbf{p})} a_M^\dagger(\mathbf{p}, +) \right). \quad (4.7)$$

Recall the normalization factor is $N(\mathbf{p}) = E(\mathbf{p}) + |\mathbf{p}|$. To proceed we point out that the operator relations can be rewritten as a rotation between a definite lepton family number state and mixed state. To accomplish the rotation we use the velocity definitions $|\mathbf{p}|/E(\mathbf{p}) = v$ and $m/E(\mathbf{p}) = \sqrt{1 - v^2}$;

$$\cosh \theta_p = \frac{\sqrt{1 + v}}{\sqrt{2v}}, \quad (4.8)$$

$$\sinh \theta_p = \frac{\sqrt{1 - v}}{\sqrt{2v}}. \quad (4.9)$$

The angle of rotation θ_p depends on the momentum of the particle states. Then, we rewrite the operator relations as rotations dependent on the angle θ_p ;

$$\begin{pmatrix} a(\mathbf{p}) \\ a^\dagger(-\mathbf{p}) \end{pmatrix} = v \begin{pmatrix} \cosh \theta_p & i \sinh \theta_p \\ i \sinh \theta_p & \cosh \theta_p \end{pmatrix} \begin{pmatrix} a_M(\mathbf{p}, -) \\ a_M^\dagger(-\mathbf{p}, -) \end{pmatrix}, \quad (4.10)$$

$$\begin{pmatrix} b(\mathbf{p}) \\ b^\dagger(-\mathbf{p}) \end{pmatrix} = v \begin{pmatrix} \cosh \theta_p & i \sinh \theta_p \\ i \sinh \theta_p & \cosh \theta_p \end{pmatrix} \begin{pmatrix} a_M(\mathbf{p}, +) \\ a_M^\dagger(-\mathbf{p}, +) \end{pmatrix}. \quad (4.11)$$

To further simplify we use the hyperbolic trig relation of $\cosh 2x = \sinh^2 x + \cosh^2 x$, which leads to $\cosh 2\theta_p = v^{-1} = \cos^{-1} 2\phi_p$. Then Eq.(4.10) and Eq.(4.11) are written as,

$$\begin{pmatrix} a(\mathbf{p}) \\ a^\dagger(-\mathbf{p}) \end{pmatrix} = n_p \begin{pmatrix} \cos \phi_p & i \sin \phi_p \\ i \sin \phi_p & \cos \phi_p \end{pmatrix} \begin{pmatrix} a_M(\mathbf{p}, -) \\ a_M^\dagger(-\mathbf{p}, -) \end{pmatrix}, \quad (4.12)$$

$$\begin{pmatrix} b(\mathbf{p}) \\ b^\dagger(-\mathbf{p}) \end{pmatrix} = n_p \begin{pmatrix} \cos \phi_p & i \sin \phi_p \\ i \sin \phi_p & \cos \phi_p \end{pmatrix} \begin{pmatrix} a_M(\mathbf{p}, +) \\ a_M^\dagger(-\mathbf{p}, +) \end{pmatrix}, \quad (4.13)$$

where $n_p = \sqrt{\cos 2\phi_p}$.

The momentum dependent rotation ϕ_p suggests the existence of a Bogolyubov transformation,

$$T(\phi_p) = e^{i\phi_p[g(\mathbf{p},+) + g(\mathbf{p},-)]}, \quad (4.14)$$

where the dimensionless generators of the transformation are,

$$g(\mathbf{p}, \lambda) = \frac{a_M(\mathbf{p}, \lambda)a_M(-\mathbf{p}, \lambda) + a_M^\dagger(\mathbf{p}, \lambda)a_M^\dagger(-\mathbf{p}, \lambda)}{2E(\mathbf{p})(2\pi)^3\delta^{(3)}(0)}. \quad (4.15)$$

The operator relations then become,

$$a(\mathbf{p}) = n_p T(\phi_p) a_M(\mathbf{p}, -) T^{-1}(\phi_p), \quad (4.16)$$

$$a(-\mathbf{p}) = n_p T(\phi_p) a_M(-\mathbf{p}, -) T^{-1}(\phi_p), \quad (4.17)$$

$$b(\mathbf{p}) = n_p T(\phi_p) a_M(\mathbf{p}, +) T^{-1}(\phi_p), \quad (4.18)$$

$$b(-\mathbf{p}) = n_p T(\phi_p) a_M(-\mathbf{p}, +) T^{-1}(\phi_p). \quad (4.19)$$

Because we have two sets of operators, $a(\mathbf{p})$ and $a_M(\mathbf{p}, -)$, we should define two distinct vacua. The first vacuum is annihilated by $a(\mathbf{p})$ and $b(\mathbf{p})$,

$$a(\pm\mathbf{p})|0\rangle = b(\pm\mathbf{p})|0\rangle = 0; \quad (4.20)$$

and the second vacuum is annihilated by $a_M(\mathbf{p}, -)$ and $a_M(\mathbf{p}, +)$,

$$a_M(\pm\mathbf{p}, -)|0_M\rangle = a_M(\pm\mathbf{p}, +)|0_M\rangle = 0. \quad (4.21)$$

Similar to the operators the vacua are related to each other though Eq.(4.14) the Bogolyubov transformation,

$$|0\rangle = \prod_{\mathbf{p} \in A} T(\phi_p) |0_M\rangle. \quad (4.22)$$

We expand the Bogolyubov transformation to show that the relationship between the vacua is nontrivial,

$$|0\rangle = \prod_{\mathbf{p} \in A} \left[\cos^2 \phi_p - B_M^\dagger(\mathbf{p}, +) B_M^\dagger(\mathbf{p}, -) \sin^2 \phi_p \right. \\ \left. + i \sin \phi_p \cos \phi_p \sum_{\lambda=\pm} B_M^\dagger(\mathbf{p}, \lambda) \right] |0_M\rangle. \quad (4.23)$$

The bosonic operator $B_M^\dagger(\mathbf{p}, \lambda)$ creates two Majorana particles with opposite momentum. These bosonic operators appear as a superposition of the Majorana particles in a state of two pairs or one pair with the norm,

$$\langle 0_M | B_M(\mathbf{p}, -) B_M(\mathbf{p}, +) B_M^\dagger(\mathbf{p}, +) B_M^\dagger(\mathbf{p}, -) | 0_M \rangle = 1, \quad (4.24)$$

$$\langle 0_M | \sum_{\lambda'} B_M(\mathbf{p}, \lambda') \sum_{\lambda} B_M^\dagger(\mathbf{p}, \lambda) | 0_M \rangle = 2, \quad (4.25)$$

$$B_M^\dagger(\mathbf{p}, \lambda) = \frac{a_M^\dagger(-\mathbf{p}, \lambda) a_M^\dagger(\mathbf{p}, \lambda)}{2E(\mathbf{p})(2\pi)^3 \delta^{(3)}(0)}. \quad (4.26)$$

4.3 Expectation value in the Schrödinger picture

We use three steps to calculate the Majorana expectation value in the Schrödinger picture. We start with an initial state of definite lepton number, then we solve for the evolution form of that state, and last we sandwich that state around the operator for the lepton family number. The initial state is built using Eq.(4.23) the relationship between the vacua and Eq.(4.16) the transformation of operator,

$$|\Psi(t=0)\rangle = \frac{a^\dagger(\mathbf{q})|0\rangle}{\sqrt{2|\mathbf{q}|(2\pi)^3\delta^{(3)}(0)}}, \quad (4.27)$$

which becomes,

$$\begin{aligned} |\Psi(0)\rangle = & \prod_{(\mathbf{p} \neq \mathbf{q}) \in A} \left[\cos^2 \phi_p - B_M^\dagger(\mathbf{p}, +)B_M^\dagger(\mathbf{p}, -) \sin^2 \phi_p \right. \\ & \left. + i \sin \phi_p \cos \phi_p \sum_{\lambda=\pm} B_M^\dagger(\mathbf{p}, \lambda) \right] \\ & \times \sqrt{\frac{\cos 2\phi_q}{2|\mathbf{q}|(2\pi)^3\delta^{(3)}(0)}} \left[(\cos \phi_q \right. \\ & \left. + iB_M^\dagger(\mathbf{q}, +) \sin \phi_q) a_M^\dagger(\mathbf{q}, -) \right] |0_M\rangle. \end{aligned} \quad (4.28)$$

Next we obtain the time evolution form,

$$|\Psi(t)\rangle = \frac{1}{\sqrt{2|\mathbf{q}|(2\pi)^3\delta^{(3)}(0)}} e^{-iH(t)} a^\dagger(\mathbf{q})|0\rangle; \quad (4.29)$$

which is equivalent to,

$$\begin{aligned} |\Psi(t)\rangle = & \prod_{(\mathbf{p} \neq \mathbf{q}) \in A} \left[\cos^2 \phi_p - B_M^\dagger(\mathbf{p}, +)B_M^\dagger(\mathbf{p}, -) \sin^2 \phi_p e^{-4iE(\mathbf{p})t} \right. \\ & \left. + i \sin \phi_p \cos \phi_p e^{-2iE(\mathbf{p})t} \sum_{\lambda=\pm} B_M^\dagger(\mathbf{p}, \lambda) \right] \\ & \times e^{-iE(\mathbf{q})t} \sqrt{\frac{\cos 2\phi_q}{2|\mathbf{q}|(2\pi)^3\delta^{(3)}(0)}} \left[(\cos \phi_q \right. \\ & \left. + i e^{-2iE(\mathbf{q})t} B_M^\dagger(\mathbf{q}, +) \sin \phi_q) a_M^\dagger(\mathbf{q}, -) \right] |0_M\rangle. \end{aligned} \quad (4.30)$$

Lastly, we sandwich Eq.(4.30) the time evolution form of the initial state around the operator for the lepton family number. For the single flavor case we define the operator for the lepton family number to be,

$$L^S = \int' \frac{d\mathbf{q}}{(2\pi)^3 2|\mathbf{q}|} (a^\dagger(\mathbf{q})a(\mathbf{q}) - b^\dagger(\mathbf{q})b(\mathbf{q})). \quad (4.31)$$

We use the results of the Bogolyubov transformation in Eq.(4.16), Eq.(4.17), Eq.(4.18), and Eq.(4.19) to substitute the operators,

$$L^S = \int_{\mathbf{q} \in A} \frac{V d\mathbf{q}}{(2\pi)^3} \sum_{\lambda=\pm} (-\lambda) \left[v (A(\mathbf{q}, \lambda) + A(-\mathbf{q}, \lambda)) - i\sqrt{1-v^2} \left(B_M^\dagger(\mathbf{q}, \lambda) + B_M(\mathbf{q}, -\lambda) \right) \right]. \quad (4.32)$$

The notation $V = (2\pi)^3 \delta^{(3)}(0)$ refers to a volume normalization and we define,

$$A(\mathbf{q}, \lambda) = \frac{a_M^\dagger(\mathbf{p}, \lambda) a_M(\mathbf{p}, \lambda)}{2E(\mathbf{p})(2\pi)^3 \delta^{(3)}(0)}. \quad (4.33)$$

Sandwiching the operator of Eq.(4.32) with Eq.(4.30) the evolved initial state results in two matrix element calculations,

$$\begin{aligned} \langle L^S \rangle = & \prod_{(\mathbf{p} \neq \mathbf{q}) \in A} \langle 0_M | \left[\cos^2 \phi_p - B_M(\mathbf{p}, +) B_M(\mathbf{p}, -) \sin^2 \phi_p e^{4iE(\mathbf{p})t} \right. \\ & \left. - i \sin \phi_p \cos \phi_p e^{2iE(\mathbf{p})t} \sum_{\lambda=\pm} B_M(\mathbf{p}, \lambda) \right] \\ & \times \left[\cos^2 \phi_p - B_M^\dagger(\mathbf{p}, +) B_M^\dagger(\mathbf{p}, -) \sin^2 \phi_p e^{-4iE(\mathbf{p})t} \right. \\ & \left. + i \sin \phi_p \cos \phi_p e^{-2iE(\mathbf{p})t} \sum_{\lambda=\pm} B_M^\dagger(\mathbf{p}, \lambda) \right] |0_M \rangle \\ & \times \int_{\mathbf{q} \in A} \frac{d\mathbf{q}}{2|\mathbf{q}|(2\pi)^3} \cos 2\phi_q \langle 0_M | a_M(\mathbf{q}, -) \\ & \times [\cos \phi_q - i e^{2iE(\mathbf{q})t} B_M(\mathbf{q}, +) \sin \phi_q] \ell^S \\ & \times [\cos \phi_q + i e^{-2iE(\mathbf{q})t} B_M^\dagger(\mathbf{q}, +) \sin \phi_q] a_M^\dagger(\mathbf{q}, -) |0_M \rangle. \end{aligned} \quad (4.34)$$

The first matrix element consists of the direct product for all momentum $(\mathbf{p} \neq \mathbf{q}) \in A$ and is equal to one. The second matrix element is the integral over $\mathbf{q} \in A$, which evaluates to be,

$$\langle L^f \rangle = v^2 + (1 - v^2) \cos 2E(\mathbf{q})t. \quad (4.35)$$

Thus, our result in the Schrödinger picture is exactly the same as the Heisenberg picture for the single flavor case derived in section 2.1.

Chapter 5

Conclusions

Neutrino physics has evolved significantly since the discovery of flavor oscillations by Super Kamiokande [50] and the Sudbury Neutrino Observatory [51]. Nowadays, there are numerous experiments that aim to take precision measurements within the next ten years. Some measurements include:

- Neutrino mass hierarchy,
- Neutrino mass type,
- CP violation in the leptonic sector,
- Absolute mass scale of the neutrinos.

Furthermore, the originating work of Pontecovo with neutrino oscillations in quantum mechanics [47] has been established to not be a theoretically complete model for neutrino oscillations. A consensus for the theory of neutrino oscillations in quantum field theory has not been reached and is an active area of research [67, 68, 69, 70, 71, 72, 74, 73, 75, 76, 77, 78, 79, 80, 81, 82, 83].

We developed a formulation of neutrino flavor oscillations based on lepton family numbers in quantum field theory. We introduced lepton family numbers in section 1.1.2 as conserved values in $V - A$ theory and a $U(1)$ global symmetry in the Standard Model. However, neutrino flavor oscillations imply lepton family numbers are violated [8]. We started with a derivation of lepton family number for neutrinos with Majorana masses in sections 2.1 and 2.2. The main result of that derivation is the Majorana expectation value of Eq.(2.58) from our original work [86]. Some important features of the Majorana expectation value are,

- The cosine and sine terms are responsible for time dependent oscillations of the expectation value.
- In the last line of the equation, the quantity $\text{Re}(U_{\alpha k}^* U_{\sigma k}^* U_{\alpha j} U_{\sigma j})$ is dependent on the Majorana phases α_{21} and α_{31} . Those Majorana phases are observable CP phases and could be determined by some experiments.
- A sum over all the lepton family numbers $\sum_{\alpha} \langle \sigma(\mathbf{q}) | L_{\alpha}^M(t) | \sigma(\mathbf{q}) \rangle$ is the total lepton number. The total lepton number is not a conserved, time independent, value because of the minus sign in the last term. We explored this further in section 3.1.
- The quantum mechanics equation for neutrino flavor oscillation Eq.(1.13) is recovered from Eq.(2.58), the Majorana expectation value, using the ultra-relativistic limit; which we discussed in section 2.2.2.

Next, we derived the lepton family number for neutrinos with Dirac masses in section 2.3. Our second main result is the Dirac expectation value Eq.(2.127) that we derived in section 2.3 and is new for this thesis. The discussion we had in section 2.2.2 about the comparison between the Majorana expectation value and quantum mechanic formulation also applies to the Dirac expectation value. This is because the lines one though four match exactly between Eq.(2.58) the Majorana expectation value and Eq.(2.127) the Dirac expectation value, and the last line is suppressed by the absolute masses of the neutrinos.

In chapter 3, we have illustrated how our formulation provides a look into if neutrinos are Majorana or Dirac fermions. This is a new comparison for this thesis. We accomplished this by investigating differences in the evolution of the Majorana expectation value Eq.(2.58) and the Dirac expectation value Eq.(2.127). We investigated those differences in two ways, first by studying the total lepton number and second by comparing the low momentum phenomenology. For total lepton number, the Dirac expectation value was found to conserve total lepton number, whereas the Majorana expectation value was found to violate total lepton number. We highlighted how this occurs though figure 3.1 and illustrated the effect on disappearance and appearance calculations in figures 3.2 and 3.3. For the low momentum phenomenology we discussed how our formulation has three interesting phenomenology properties,

1. we can distinguish the neutrino mass type,

2. differences from the neutrino mass hierarchy are enhanced,
3. the Majorana phases can play an important role to the Majorana Expectation value.

For the final chapter, chap. 4, we discussed some theoretical properties of our model, and proved our formulation is the same in the Schrödinger and Heisenberg pictures [95]. We were motivated to do this because our creation and annihilation operators of Eq.(2.46) and Eq.(2.47), Eq.(2.52) and Eq.(2.53), Eq.(2.97) through Eq.(2.100), and finally Eq.(2.107) through Eq.(2.110), have a non-trivial mixing. That suggests a non-trivial relationship between the Fock spaces of the operators, which is not usually considered in high energy physics. When we reformulated to the Schrödinger picture, we found the operator relations of Eq.(2.46) and Eq.(2.47) from the Majorana calculation can be expressed as a Bogolyubov transformation. That was similar to Thermal field theory and gave an interesting theoretical background to our model. This concludes the main chapters of this thesis.

Acknowledgements

I cannot begin to express my thanks to my supervisor Takuya Morozumi, who has supported me in my research and personal endeavors over the last three years. He has also always challenged me to become a better physicist, student, and person. I would also like to express my gratitude to Apriadi Salim Adam, Yuta Kawamura, Yamato Matsuo, Yusuke Shimizu, Yuya Tokunaga, and Naoya Toyota, my collaborators on the article that this work is based on, for there countless insights. I am very grateful for the discussions with Kei Yamamoto, Keiko I. Nagao, and Hiroyuki Takata about Elementary Particle Physics and Mathematics. I would also like to acknowledge the help of Tomohiro Inagaki, Chiho Nonaka and Ken-Ichi Ishikawa the staff members of the Theoretical Particle and Hadron Physics Group at Hiroshima University. In addition, I am very grateful to students in the Theoretical Particle and Hadron Physics Group at Hiroshima University for their support. In particular, I am very grateful to the initial support from Yuta Kawamura, Yamato Matsuo, and Kenta Takagi after moving to Japan.

I would like to extend my deepest gratitude to my parents and grandparents, all of whom have supported me and continue to support me on my sometimes crazy endeavors. I must also thank the

members and staff of Hiroshima International Plaza, Sachiyo Nose from the student health center; and Kaori Kusaka, Tomoko Sato, Kiyo Mondo, Kozue Akimura, and Ms Hata from the Graduate School of Science support offices. Finally, I would like to thank the Japan Student Services Organization (JASSO) and the Japanese government Ministry of Education, Culture, Sports, Science and Technology (MEXT) for the financial support to be able to preform my studies and research.

Appendix A

Parameterization of the unitary mixing matrix

The Pontecorvo, Maki, Nakagawa, and Sakata (PMNS) mixing matrix is an important piece of neutrino flavor oscillations. As such, we give a brief overview of the topic with more details in the references [8, 101, 102]. The origin of the PMNS matrix is the same as the CKM matrix of the quark sector. We start with Eq.(1.3) the charged current of the weak interaction, which we reproduce here,

$$\mathcal{L}_{\nu,l}^{CC} = - \sum_{\alpha} \frac{g}{2\sqrt{2}} (\bar{\nu}_{\alpha L} \gamma^{\rho} l_{\alpha L} W_{\rho} + \text{h.c.}). \quad (\text{A.1})$$

The lepton mass term written as,

$$\mathcal{L}_l^M = -(\bar{l}_{\alpha R} M_l l_{\alpha L} + \text{h.c.}) - \mathcal{L}_l^{M\nu} \quad (\text{A.2})$$

where charged leptons obtain a mass through the Standard Model Higgs mechanism, and the neutrinos obtain a mass through some beyond the Standard Model physics. In the interaction basis the charged lepton mass matrix M_l is not diagonal. We can diagonalize the charged lepton mass matrix with two unitary matrices,

$$(W^{l\dagger})_{i\alpha} (M_l)_{\alpha\beta} (V^l)_{\beta j} = (m_l)_i \delta_{ij}, \quad (\text{A.3})$$

where W^l comes from the right-handed charged leptons and V^l from the left-handed.

A similar process happens for the neutrinos, but the details of the two unitary matrices depends on if the neutrinos have a Dirac or Majorana mass term. Regardless if neutrinos have Dirac or Majorana

mass, the charged current of the weak interaction is left-handed, so the interaction basis is the most convenient. Then in the interaction basis, the unitary matrices we used to diagonalize the lepton mass matrices modify the charged current Lagrangian,

$$\mathcal{L}_{\nu I}^{CC} = - \sum_{k,j} (V_{\alpha k}^\nu)^\dagger V_{\alpha j}^l \frac{g}{2\sqrt{2}} (\bar{\nu}_{kL} \gamma^\rho l_{jL} W_\rho + \text{h.c.}); \quad (\text{A.4})$$

where the combination of the lepton and neutrino unitary matrices is the PMNS matrix,

$$U_{kj} = (V^{\nu\dagger})_{k\alpha} V_{\alpha j}^l. \quad (\text{A.5})$$

For three neutrino mass eigenstates, the PMNS matrix is a complex unitary matrix with nine real degrees of freedom. We can rotate away three degrees of freedom by re-parameterizing the charged lepton masses. Two more degrees of freedom can be re-parameterized if neutrinos have a Dirac mass, otherwise for a Majorana mass six degrees of freedom remain. The degrees of freedom are three angles θ_{12} , θ_{23} , and θ_{13} ; and three phases δ , α_{21} , and α_{31} . The last two phases of α_{21} and α_{31} are the Majorana phases, which get rotated away if neutrinos have a Dirac mass. This results in,

$$U_{\alpha k} = \begin{pmatrix} c_{12}c_{13} & s_{12}c_{13} & s_{13}e^{-i\delta} \\ -s_{12}c_{23} - c_{12}s_{23}s_{13}e^{i\delta} & c_{12}c_{23} - s_{12}s_{23}s_{13}e^{i\delta} & s_{23}c_{13} \\ s_{12}s_{23} - c_{12}c_{23}s_{13}e^{i\delta} & -c_{12}s_{23} - s_{12}c_{23}s_{13}e^{i\delta} & c_{23}c_{13} \end{pmatrix} \mathbf{U}_M, \quad (\text{A.6})$$

where the matrix holding the Majorana phases is given as,

$$\mathbf{U}_M = \begin{pmatrix} 1 & & \\ & e^{i\frac{\alpha_{21}}{2}} & \\ & & e^{i\frac{\alpha_{31}}{2}} \end{pmatrix}. \quad (\text{A.7})$$

All the mixing angles and the Dirac CP phase δ have been measured by experiments, and we use the best-fit values from the NuFITv5.0 collaboration dataset [88]. Presently it is not known if neutrinos have a Majorana mass, so no measurements of the Majorana phases have been performed.

As a short aside discussion, the quantum mechanic probability of Eq.(1.13) after the ultrarelativistic approximation suggests only the mass squared differences Δm_{kj}^2 of the neutrinos can be measured. In fact, because in all neutrino oscillation experiments the neutrinos are considered ultrarelativistic the experiments can only measure the mass squared differences. The best-fit values for the mass squared

differences are also reported by the NuFITv5.0 collaboration. Other experiments are designed to measure the lightest neutrino mass, and most recently have only provided an upper bound of $m_{eff} \leq 0.9\text{eV}$ [103]. This means for our analysis we are free to choose values for α_{21} , α_{31} , and $m_{lightest}$.

Appendix B

Regions of the momentum

We will explain the calculation of Eq.(2.44) the continuity condition, and how the regions of the momentum appear in the operators of Eq.(2.56) and Eq.(2.113) the lepton family numbers. This discussion is based on the supplemental material [104].

B.1 The continuity condition

We start with the equation of motion for Eq.(2.21) the Majorana Lagrangian,

$$\gamma_\mu \partial^\mu \psi_{L\alpha} = -i\theta(t)m_{\alpha\beta}^* \psi_{L\alpha}^C, \quad (\text{B.1})$$

where we have suppressed the field dependence notation of $\psi_{L\alpha}(t, \mathbf{x})$ and used $\psi_{L\alpha}^C = (\psi_{L\alpha})^C$. The time derivative of the field is taken,

$$\frac{\partial}{\partial t} \nu_{L\alpha} = -\gamma^0 \gamma^i \frac{\partial}{\partial x^i} \nu_{L\alpha} - i\theta(t)m_{\alpha\beta}^* \nu_{L\beta}^C. \quad (\text{B.2})$$

Then we integrate both sides of the equation over an infinitesimal time region,

$$\int_{-\epsilon}^{\epsilon} dt \frac{\partial}{\partial t} \nu_{L\alpha} = - \int_{-\epsilon}^{\epsilon} dt \gamma^0 \gamma^i \frac{\partial}{\partial x^i} \nu_{L\alpha} - i \int_0^{\epsilon} dt \theta(t) m_{\alpha\beta}^* \nu_{L\beta}^C. \quad (\text{B.3})$$

After integration on the left-hand side the result is,

$$\nu_{L\alpha}(\epsilon) - \nu_{L\alpha}(-\epsilon) = - \int_{-\epsilon}^{\epsilon} dt \gamma^0 \gamma^i \frac{\partial}{\partial x^i} \nu_{L\alpha} - i \int_0^{\epsilon} dt \theta(t) m_{\alpha\beta}^* \nu_{L\beta}^C. \quad (\text{B.4})$$

Lastly, we take the limit of $\epsilon \rightarrow +0$ and use $\psi_{L\alpha} = U_{\alpha i} L \psi_i$ from Eq.(2.22) to obtain,

$$\lim_{\epsilon \rightarrow 0^+} \psi_{L\alpha}(-\epsilon, \mathbf{x}) = \lim_{\epsilon \rightarrow 0^+} U_{\alpha i} L \psi_i(+\epsilon, \mathbf{x}), \quad (\text{B.5})$$

which is the same as Eq.(2.45). A similar derivation occurs for the Dirac mass case. This forms our continuity condition.

B.2 The momentum regions

There is a subtle point about the momentum of the neutrinos that is important to understand our derivation for the operators of Eq.(2.56) and Eq.(2.113) the lepton family numbers. The fields on the left-hand side of Eq.(B.5) the continuity condition are Weyl fields. Thus, the fields $\psi_{L\alpha}(-\epsilon, \mathbf{x})$ can not have zero momentum. The continuity condition implies the Majorana or Dirac fields also do not have zero momentum, despite the fact zero momentum is possible for a free Majorana or Dirac field. Then, we split the momentum into two regions denoted A and \bar{A} with the direction of the momentum defined as,

$$\mathbf{n} = \frac{\mathbf{p}}{|\mathbf{p}|}, \quad \{\mathbf{p} : \mathbf{p} \neq 0\}. \quad (\text{B.6})$$

The direction of the momentum \mathbf{n} can be parameterized by two polar angles θ and ϕ . This places the hemisphere of region A inside the angle $\phi = [0, \pi)$ and the hemisphere of region \bar{A} inside $\phi = [\pi, 2\pi)$. The angle θ is always $[0, 2\pi)$ no matter the hemisphere. So, to bring operators from region \bar{A} to region A we rotate them accordingly with \mathbf{n} .

Bibliography

- [1] K. Abe *et al.* [Super-Kamiokande], Phys. Rev. D **94**, no.5, 052010 (2016) doi:10.1103/PhysRevD.94.052010 [arXiv:1606.07538 [hep-ex]].
- [2] K. Abe *et al.* [Super-Kamiokande], Phys. Rev. D **97**, no.7, 072001 (2018) doi:10.1103/PhysRevD.97.072001 [arXiv:1710.09126 [hep-ex]].
- [3] M. Jiang *et al.* [Super-Kamiokande], PTEP **2019**, no.5, 053F01 (2019) doi:10.1093/ptep/ptz015 [arXiv:1901.03230 [hep-ex]].
- [4] P. Adamson *et al.* [NOvA], Phys. Rev. Lett. **116**, no.15, 151806 (2016) doi:10.1103/PhysRevLett.116.151806 [arXiv:1601.05022 [hep-ex]].
- [5] M. A. Acero *et al.* [NOvA], Phys. Rev. D **98**, 032012 (2018) doi:10.1103/PhysRevD.98.032012 [arXiv:1806.00096 [hep-ex]].
- [6] M. A. Acero *et al.* [NOvA], Phys. Rev. Lett. **123**, no.15, 151803 (2019) doi:10.1103/PhysRevLett.123.151803 [arXiv:1906.04907 [hep-ex]].
- [7] J. Schneps, AIP Conf. Proc. **1666**, no.1, 190002 (2015) doi:10.1063/1.4915603
- [8] C. Giunti and C. W. Kim, “Fundamentals of Neutrino Physics and Astrophysics,”
- [9] M. Fukugita and T. Yanagida, “Physics of neutrinos and applications to astrophysics,” doi:10.1007/978-3-662-05119-1
- [10] J. Chadwick, Verh. Phys. Gesell. **16**, 383-391 (1914)
- [11] C. D. Ellis and W. A. Wooster, Proc. Roy. Soc. Lond. A **117**, no.776, 109-123 (1927) doi:10.1098/rspa.1927.0168
- [12] W. Pauli, “Dear radioactive ladies and gentlemen,”

- [13] E. Fermi, Ric. Sci. **4**, 491-495 (1933)
- [14] H. Bethe and R. Peierls, Nature **133**, 532 (1934)
doi:10.1038/133532a0
- [15] B. Pontecorvo, Report PD-205 of the National Research Council of Canada, Division of Atomic Energy, Chalk River, Ontario, Nov. 13, 1946.
- [16] C. L. Cowan, F. Reines, F. B. Harrison, H. W. Kruse and A. D. McGuire, Science **124**, 103-104 (1956)
doi:10.1126/science.124.3212.103
- [17] E. Fermi, Z. Phys. **88**, 161-177 (1934) doi:10.1007/BF01351864
- [18] G. Gamow and E. Teller, Phys. Rev. **51**, 289-289 (1937)
doi:10.1103/PhysRev.51.289
- [19] B. Pontecorvo, Phys. Rev. **72**, 246 (1947)
doi:10.1103/PhysRev.72.246
- [20] C. S. Wu, E. Ambler, R. W. Hayward, D. D. Hoppes and R. P. Hudson, Phys. Rev. **105**, 1413-1414 (1957) doi:10.1103/PhysRev.105.1413
- [21] E. Ambler, R. W. Hayward, D. D. Hoppes, R. P. Hudson and C. S. Wu, Phys. Rev. **106**, 1361-1363 (1957) doi:10.1103/PhysRev.106.1361
- [22] R. P. Feynman and M. Gell-Mann, Phys. Rev. **109**, 193-198 (1958)
doi:10.1103/PhysRev.109.193
- [23] E. C. G. Sudarshan and R. e. Marshak, Phys. Rev. **109**, 1860-1860 (1958) doi:10.1103/PhysRev.109.1860.2
- [24] J. J. Sakurai, Nuovo Cim. **7**, 649-660 (1958) doi:10.1007/BF02781569
- [25] A. Salam, Nuovo Cim. **5**, 299-301 (1957) doi:10.1007/BF02812841
- [26] L. D. Landau, Nucl. Phys. **3**, 127-131 (1957) doi:10.1016/0029-5582(57)90061-5
- [27] T. D. Lee and C. N. Yang, Phys. Rev. **105**, 1671-1675 (1957)
doi:10.1103/PhysRev.105.1671
- [28] G. Puppi, Nuovo Cim. **5**, 587-588 (1948) doi:10.1007/BF02780913
- [29] O. Klein, Nature **161**, 897-899 (1948) doi:10.1038/161897a0

- [30] T. D. Lee, M. Rosenbluth and C. N. Yang, Phys. Rev. **75**, 905 (1949) doi:10.1103/PhysRev.75.905
- [31] J. Tiomno and J. A. Wheeler, Rev. Mod. Phys. **21**, 144-152 (1949) doi:10.1103/RevModPhys.21.144
- [32] E. J. Konopinski and H. M. Mahmoud, Phys. Rev. **92**, 1045-1049 (1953) doi:10.1103/PhysRev.92.1045
- [33] G. Danby, J. M. Gaillard, K. A. Goulianos, L. M. Lederman, N. B. Mistry, M. Schwartz and J. Steinberger, Phys. Rev. Lett. **9**, 36-44 (1962) doi:10.1103/PhysRevLett.9.36
- [34] B. Pontecorvo, Zh. Eksp. Teor. Fiz. **37**, 1751-1757 (1959)
- [35] S. L. Glashow, Nucl. Phys. **22**, 579-588 (1961) doi:10.1016/0029-5582(61)90469-2
- [36] S. Weinberg, Phys. Rev. Lett. **19**, 1264-1266 (1967) doi:10.1103/PhysRevLett.19.1264
- [37] A. Salam, Conf. Proc. C **680519**, 367-377 (1968) doi:10.1142/9789812795915_0034
- [38] F. J. Hasert, H. Faissner, W. Krenz, J. Von Krogh, D. Lanske, J. Morfin, K. Schultze, H. Weerts, G. H. Bertrand-Coremans and J. Lemonne, *et al.* Phys. Lett. B **46**, 121-124 (1973) doi:10.1016/0370-2693(73)90494-2
- [39] F. J. Hasert *et al.* [Gargamelle Neutrino], Phys. Lett. B **46**, 138-140 (1973) doi:10.1016/0370-2693(73)90499-1
- [40] F. J. Hasert *et al.* [Gargamelle Neutrino], Nucl. Phys. B **73**, 1-22 (1974) doi:10.1016/0550-3213(74)90038-8
- [41] S. Schael *et al.* [ALEPH, DELPHI, L3, OPAL, SLD, LEP Electroweak Working Group, SLD Electroweak Group and SLD Heavy Flavour Group], Phys. Rept. **427**, 257-454 (2006) doi:10.1016/j.physrep.2005.12.006 [arXiv:hep-ex/0509008 [hep-ex]].
- [42] B. T. Cleveland, T. Daily, R. Davis, Jr., J. R. Distel, K. Lande, C. K. Lee, P. S. Wildenhain and J. Ullman, Astrophys. J. **496**, 505-526 (1998) doi:10.1086/305343

- [43] A. B. McDonald, Rev. Mod. Phys. **88**, no.3, 030502 (2016)
doi:10.1103/RevModPhys.88.030502
- [44] T. Kajita, Rev. Mod. Phys. **88**, no.3, 030501 (2016)
doi:10.1103/RevModPhys.88.030501
- [45] B. Pontecorvo, Sov. Phys. JETP **6**, 429 (1957)
- [46] B. Pontecorvo, Zh. Eksp. Teor. Fiz. **34**, 247 (1957)
- [47] B. Pontecorvo, Zh. Eksp. Teor. Fiz. **53**, 1717-1725 (1967)
- [48] V. N. Gribov and B. Pontecorvo, Phys. Lett. B **28**, 493 (1969)
doi:10.1016/0370-2693(69)90525-5
- [49] Z. Maki, M. Nakagawa and S. Sakata, Prog. Theor. Phys. **28**, 870-880
(1962) doi:10.1143/PTP.28.870
- [50] Y. Fukuda *et al.* [Super-Kamiokande], Phys. Rev. Lett. **81**,
1562-1567 (1998) doi:10.1103/PhysRevLett.81.1562 [arXiv:hep-
ex/9807003 [hep-ex]].
- [51] Q. R. Ahmad *et al.* [SNO], Phys. Rev. Lett. **89**, 011301 (2002)
doi:10.1103/PhysRevLett.89.011301 [arXiv:nucl-ex/0204008 [nucl-
ex]].
- [52] L. Wolfenstein, Phys. Rev. D **17**, 2369-2374 (1978)
doi:10.1103/PhysRevD.17.2369
- [53] S. P. Mikheev and A. Y. Smirnov, Nuovo Cim. C **9**, 17-26 (1986)
doi:10.1007/BF02508049
- [54] S. P. Mikheyev and A. Y. Smirnov, Sov. J. Nucl. Phys. **42**, 913-917
(1985)
- [55] B. Kayser, Phys. Rev. D **24**, 110 (1981) doi:10.1103/PhysRevD.24.110
- [56] C. Giunti and C. W. Kim, Found. Phys. Lett. **14**, no.3, 213-229 (2001)
doi:10.1023/A:1012230026160 [arXiv:hep-ph/0011074 [hep-ph]].
- [57] S. Eliezer and A. R. Swift, Nucl. Phys. B **105**, 45-51 (1976)
doi:10.1016/0550-3213(76)90059-6
- [58] S. M. Bilenky and B. Pontecorvo, Yad. Fiz. **24**, 603-608 (1976)

- [59] S. M. Bilenky and B. Pontecorvo, *Lett. Nuovo Cim.* **17**, 569 (1976)
doi:10.1007/BF02746567
- [60] R. G. Winter, *Lett. Nuovo Cim.* **30**, 101-104 (1981)
doi:10.1007/BF02817319
- [61] C. Giunti, C. W. Kim and U. W. Lee, *Phys. Rev. D* **45**, 2414-2420
(1992) doi:10.1103/PhysRevD.45.2414
- [62] E. Akhmedov, *JHEP* **07**, 070 (2017) doi:10.1007/JHEP07(2017)070
[arXiv:1703.08169 [hep-ph]].
- [63] E. K. Akhmedov and A. Y. Smirnov, *Phys. Atom. Nucl.* **72**, 1363-1381
(2009) doi:10.1134/S1063778809080122 [arXiv:0905.1903 [hep-ph]].
- [64] E. Akhmedov, “Quantum mechanics aspects and subtleties of
neutrino oscillations,” [arXiv:1901.05232 [hep-ph]].
- [65] D. Bohm, “Quantum Theory,”
- [66] S. Weinberg, “The Quantum theory of fields. Vol. 1: Foundations,”
- [67] M. Zralek, *Acta Phys. Polon. B* **29**, 3925-3956 (1998) [arXiv:hep-ph/9810543 [hep-ph]].
- [68] M. Beuthe, *Phys. Rept.* **375**, 105-218 (2003) doi:10.1016/S0370-1573(02)00538-0 [arXiv:hep-ph/0109119 [hep-ph]].
- [69] C. Giunti, C. W. Kim, J. A. Lee and U. W. Lee, *Phys. Rev. D* **48**, 4310-4317 (1993) doi:10.1103/PhysRevD.48.4310 [arXiv:hep-ph/9305276 [hep-ph]].
- [70] C. Giunti, C. W. Kim and U. W. Lee, *Phys. Lett. B* **421**, 237-244 (1998) doi:10.1016/S0370-2693(98)00014-8 [arXiv:hep-ph/9709494 [hep-ph]].
- [71] K. Kiers and N. Weiss, *Phys. Rev. D* **57**, 3091-3105 (1998) doi:10.1103/PhysRevD.57.3091 [arXiv:hep-ph/9710289 [hep-ph]].
- [72] C. Y. Cardall, *Phys. Rev. D* **61**, 073006 (2000) doi:10.1103/PhysRevD.61.073006 [arXiv:hep-ph/9909332 [hep-ph]].

- [73] M. Beuthe, Phys. Rev. D **66**, 013003 (2002) doi:10.1103/PhysRevD.66.013003 [arXiv:hep-ph/0202068 [hep-ph]].
- [74] C. Giunti, JHEP **11**, 017 (2002) doi:10.1088/1126-6708/2002/11/017 [arXiv:hep-ph/0205014 [hep-ph]].
- [75] Y. V. Shtanov, Phys. Rev. D **57**, 4418-4428 (1998) doi:10.1103/PhysRevD.57.4418 [arXiv:hep-ph/9706378 [hep-ph]].
- [76] Y. Srivastava, A. Widom and E. Sassaroli, Z. Phys. C **66**, 601-605 (1995) doi:10.1007/BF01579634
- [77] Y. Srivastava, A. Widom and E. Sassaroli, Eur. Phys. J. C **2**, 769-774 (1998) doi:10.1007/s100520050181
- [78] M. Blasone, A. Capolupo and G. Vitiello, Phys. Rev. D **66**, 025033 (2002) doi:10.1103/PhysRevD.66.025033 [arXiv:hep-th/0204184 [hep-th]].
- [79] M. Blasone, A. Capolupo, O. Romei and G. Vitiello, Phys. Rev. D **63**, 125015 (2001) doi:10.1103/PhysRevD.63.125015 [arXiv:hep-ph/0102048 [hep-ph]].
- [80] M. Blasone, P. A. Henning and G. Vitiello, Phys. Lett. B **451**, 140-145 (1999) doi:10.1016/S0370-2693(99)00155-0 [arXiv:hep-th/9803157 [hep-th]].
- [81] M. Blasone, P. Jizba and G. Vitiello, Phys. Lett. B **517**, 471-475 (2001) doi:10.1016/S0370-2693(01)00985-6 [arXiv:hep-th/0103087 [hep-th]].
- [82] C. R. Ji and Y. Mishchenko, Phys. Rev. D **64**, 076004 (2001) doi:10.1103/PhysRevD.64.076004 [arXiv:hep-ph/0105094 [hep-ph]].
- [83] C. R. Ji and Y. Mishchenko, Phys. Rev. D **65**, 096015 (2002) doi:10.1103/PhysRevD.65.096015 [arXiv:hep-ph/0201188 [hep-ph]].
- [84] S. M. Bilenky and C. Giunti, Int. J. Mod. Phys. A **16**, 3931-3949 (2001) doi:10.1142/S0217751X01004967 [arXiv:hep-ph/0102320 [hep-ph]].

- [85] T. Hahn, [arXiv:physics/0607103 [physics]].
- [86] A. S. Adam, N. J. Benoit, Y. Kawamura, Y. Matsuo, T. Morozumi, Y. Shimizu, Y. Tokunaga and N. Toyota, PTEP **2021**, 5 (2021) doi:10.1093/ptep/ptab025 [arXiv:2101.07751 [hep-ph]].
- [87] M. Born, Z. Phys. **37**, no.12, 863-867 (1926) doi:10.1007/BF01397477
- [88] I. Esteban, M. C. Gonzalez-Garcia, M. Maltoni, T. Schwetz and A. Zhou, JHEP **09**, 178 (2020) doi:10.1007/JHEP09(2020)178 [arXiv:2007.14792 [hep-ph]].
- [89] B. Kayser and R. E. Shrock, Phys. Lett. B **112**, 137-142 (1982) doi:10.1016/0370-2693(82)90314-8
- [90] B. Kayser, Phys. Rev. D **26**, 1662 (1982) doi:10.1103/PhysRevD.26.1662
- [91] B. Kayser and A. S. Goldhaber, Phys. Rev. D **28**, 2341 (1983) doi:10.1103/PhysRevD.28.2341
- [92] B. Kayser, F. Gibrat-Debu and F. Perrier, World Sci. Lect. Notes Phys. **25**, 1-117 (1989)
- [93] B. Kayser, [arXiv:hep-ph/9703294 [hep-ph]].
- [94] S. Abe *et al.* [KamLAND-Zen], [arXiv:2203.02139 [hep-ex]].
- [95] N. J. Benoit, Y. Kawamura and T. Morozumi, [arXiv:2204.00971 [hep-ph]].
- [96] A. Tureanu, Eur. Phys. J. C **80**, no.1, 68 (2020) doi:10.1140/epjc/s10052-020-7628-0 [arXiv:1902.01232 [hep-ph]].
- [97] M. Blasone and L. Smaldone, Mod. Phys. Lett. A **35**, no.38, 2050313 (2020) doi:10.1142/S0217732320503137 [arXiv:2004.04739 [hep-ph]].
- [98] H. Umezawa, H. Matsumoto and M. Tachiki, "THERMO FIELD DYNAMICS AND CONDENSED STATES,"
- [99] L.E. Ballentine, "Quantum Mechanics A Modern Development,"
- [100] R. Haag Z.Naturforsch. **10** (1955) 752 doi:10.1515/zna-1955-9-1014

-
- [101] M. D. Schwartz, “Quantum Field Theory and the Standard Model,”
- [102] R.L. Workman *et al.* [Particle Data Group], PTEP **2022**, 083C01 (2022)
- [103] M. Aker *et al.* [KATRIN], Nature Phys. **18**, no.2, 160-166 (2022) doi:10.1038/s41567-021-01463-1 [arXiv:2105.08533 [hep-ex]].
- [104] A. S. Adam, N. J. Benoit, Y. Kawamura, Y. Mastuo, T. Morozumi, Y. Shimizu, Y. Tokunaga and N. Toyota, doi:10.31526/ACP.BSM-2021.29 [arXiv:2105.04306 [hep-ph]].